

Article

Two-Stage Organic Acid Leaching of Industrially Sourced LFP- and NMC-Containing Black Mass

Marc Simon Henderson ^{1,2}, Chau Chun Beh ¹, Elsayed A. Oraby ¹ and Jacques Eksteen ^{1,2,*}

¹ Western Australian School of Mines: Minerals, Energy and Chemical Engineering, Curtin University, Perth, WA 6102, Australia; marcsimon.henderson@postgrad.curtin.edu.au (M.S.H.); jane.beh@curtin.edu.au (C.C.B.); elsayed.oraby@curtin.edu.au (E.A.O.)

² Future Battery Industries Cooperative Research Centre, Perth, WA 6102, Australia

* Correspondence: jacques.eksteen@curtin.edu.au

Abstract

Over the next 5–10 years, the feedstock to lithium-ion battery recycling facilities will shift from Co- and Ni-rich chemistries to lower-value battery chemistries, such as lithium iron phosphate (LFP). Traditional recycling processes use toxic and corrosive inorganic acids for leaching, generating toxic waste streams. The low-value feedstocks will be LFP-rich with contamination from lithium cobalt oxide (LCO) and lithium–nickel–manganese–cobalt oxide (NMC) battery chemistries. Overall, the lower-value feedstock coupled with the need to reduce environmentally damaging waste streams requires the development of robust, green leaching processes capable of selectively targeting the LFP and LCO/NMC battery chemistries. This research concluded that a first-stage oxalic acid leach could selectively extract Al, Li, and P from the industrially sourced LFP-rich black mass. When operating at the optimal conditions (0.5 M oxalic acid, 5% solids, pH 0.8, and an agitation speed of 600 rpm), >99% of the Li and P and >97% of the Al were selectively extracted after 2 h, while Mn, Fe, Cu, Ni, and Co extractions were kept relatively low, namely, at 19%, <3%, <1%, 0%, and 0%. This research also explored a second-stage leach to treat the first-stage leach residue using ascorbic acid, citric acid, and glycine. It was concluded that when leaching with glycine (30 g/L glycine, a temperature of 40 °C, an agitation speed of 600 rpm, and 2% solids at pH 9.6), that >97% of the Co, >77% of the Ni, and 41% of the Mn were extracted, while the co-extraction percentages of Cu, Fe, and Al were <27%, <4%, and <2%.



Academic Editors: Johan E. ten Elshof and Yushi He

Received: 29 August 2025

Revised: 23 October 2025

Accepted: 28 October 2025

Published: 31 October 2025

Citation: Henderson, M.S.; Beh, C.C.; Oraby, E.A.; Eksteen, J. Two-Stage Organic Acid Leaching of Industrially Sourced LFP- and NMC-Containing Black Mass. *Batteries* **2025**, *11*, 401. <https://doi.org/10.3390/batteries11110401>

Copyright: © 2025 by the authors. Licensee MDPI, Basel, Switzerland. This article is an open access article distributed under the terms and conditions of the Creative Commons Attribution (CC BY) license (<https://creativecommons.org/licenses/by/4.0/>).

1. Introduction

The demand for lithium-ion batteries (LiBs) in portable electronics, the transportation sector, and power grid infrastructure has led to growing concerns around their safe disposal and recycling once they reach their end-of-life (EOL). Currently, recycling facilities are designed to handle high-value battery chemistries such as NMCs and LCOs. Thus, there is a need to understand how the battery-recycling industry can handle large quantities of spent LFP chemistries entering or making up the bulk of the feedstock.

Currently, inorganic acids such as H_2SO_4 are used throughout the battery recycling industry. However, due to excess reagent consumption and subsequent neutralization, significant amounts of harmful effluents and waste streams are produced, which do not allow for the economic recovery and recycling of reagents. Therefore, there is a need to

identify greener lixivants, such as organic acids, that are milder, less corrosive toward materials of construction, and easier to recover (e.g., through crystallization/precipitation), enabling recycling and reuse. Several researchers have investigated the use of environmentally friendly reagents such as organic acids, particularly oxalic acid, for the leaching of spent LiBs [1–8].

Li and coworkers [1] and Sun and Qiu [3] investigated using oxalic acid to leach a range of high-value battery chemistries. Sun and Qiu [3] confirmed that Li could be selectively extracted from LiCoO₂ using 1 M oxalic acid, a temperature of 80 °C, and a solid-to-liquid ratio of 50 g/L for 2 h. Meanwhile, Li and coworkers [1] investigated the use of oxalic acid to leach a wider range of battery chemistries, namely, NMC 111, NMC 532, NMC 811, LiMn₂O₄, and LiCo_{0.95}Mn_{0.05}O₂. Li and coworkers [1] concluded that when leaching using 1 M oxalic acid, with a solid-to-liquid ratio of 10 g/L, at 95 °C for 12 h, that >90% of the Li, <0.3% of the Ni, <1.8% of the Co, and <30% of the Mn were extracted. Their research shows promise in recovering Li from different battery chemistries; however, both investigated recycling single-chemistry cathodic materials, manually separated from the other battery components, and then separated from the current collecting foil (Al). In practice, it is highly unlikely that the feedstock to a recycling facility (particularly end-of-life batteries) will consist of a single battery chemistry. There are limitations to manually dismantling spent LiBs, as the required feed rate to a recycling facility is large. At an industrial scale, it is more likely that the batteries will first be discharged and then undergo some form of shredding/grinding and sieving to create a material commonly referred to as “black mass” (BM). This BM comprises the anode, cathode, current collecting foils (Al and Cu), electrolytes and conductive salts, separators, and battery casing and housing (Fe, plastic, etc.). In recent years, more researchers have investigated the leaching of this complex BM material; however, the bulk of the research involved BM derived from high-value battery chemistries (NMC, LCO, etc.).

Mettke and Yagmurlu [7] investigated the selective recovery of Li from an NMC 622-rich BM using an oxalic acid leach. The BM used in their experiments was roasted under atmospheric conditions to remove any electrolytes or salts (LiPF₆) and destroy or alter contained solvents and plastics (e.g., separator materials and binders). However, the roasting processes changed the NMC 622 structure into individual metal oxides, which are more amenable to leaching. This research concluded that temperature had very little effect on the extraction of Li, while the concentration of oxalic acid played a significant role in Li extraction. Thus, the optimal parameters were identified to be agitation at 600 rpm, a solid-to-liquid ratio of 100 g/L, and a temperature of 20 °C for 30 min, resulting in 79.77%, 25.85%, 0.97%, 13.95%, 1.23%, and 2.85% of the Li, Al, Co, Cu, Mn, and Ni being extracted, respectively. The biggest difference from researchers such as Rouquette et al. [4] is that the Al dissolution reported by [7] was much lower, as it was determined that with higher temperatures and longer leaching times, Al precipitated out as an insoluble Al-oxalate.

Researchers such as Müller and Yagmurlu [9] investigated the synergistic effect of leaching a mixture of spent LFP and NMC 622 BM with sulfuric acid. The idea behind their research was the use of LFP material as a source of Fe²⁺, which acts as a reducing agent to improve the leachability of NMC 622 BM. It was concluded that leaching with a 1:1 molar ratio of LFP to NMC, 2 M H₂SO₄, and a solid-to-liquid ratio of 100 g/L at 60 °C for 60 min resulted in 99.1%, 98.1%, 97.2%, and 97.2% of the Li, Ni, Co, and Mn being extracted, respectively.

Zou et al. [10], similar to the work of [9], investigated the effect that the presence of LFP had on the recycling of current, dominant battery chemistries such as NMC. Initial experiments were conducted using synthetic BM (pristine NMC 111 and LFP cathodic material). Zou and coworkers [10] concluded that the addition of LFP to a H₂SO₄-NMC 111

leaching system significantly increased the extraction of Li, Ni, Co, and Mn. Zou et al. [10], too, attributed the increased metal extractions to the presence of Fe^{2+} , which acted as a reductant in the leaching system, promoting the dissolution of Ni, Mn, and Co. When leaching with 2 M H_2SO_4 , at 30 °C, with a molar ratio of LFP to NMC 111 of 0.9 for 2 h, it was proven that 100%, 100%, 92.5%, and 86.9% of the Li, Co, Mn, and Ni, respectively, could be extracted. When leaching the industrially sourced BM, Zou and coworkers [10] determined that the Li, Ni, Co, and Mn extractions were significantly higher when leaching with just H_2SO_4 than those observed when leaching the pristine NMC 111. This increase was attributed to the presence of Cu and Al, which can also act as reductants [11,12]. An important aspect to note is that the Fe^{3+} can oxidize the Cu and Al in the leaching system, causing more Fe^{2+} to be regenerated, which, in turn, promotes the dissolution of the NMC material. Overall, the optimal conditions for leaching the industrial BM were determined to be 2 M H_2SO_4 , at 60 °C, with an LFP-to-NMC BM ratio of 1:1.77 g/g for 3 h. Under optimal conditions, 100%, 100%, 100%, 95%, 91%, 87%, and 46% of the Li, Fe, Co, Cu, Mn, Ni, and Al were extracted.

The research conducted by Zou et al. [10] and Muller and Yagmurlu [9] illustrates the benefits, in certain cases, of leaching a feedstock with mixed chemistries, as in this case, the presence of LFP enhanced the leaching of the NMC material. However, the most apparent downside to their work is still the use of sulfuric acid, as it is highly corrosive, requires special handling, and often leads to the production of toxic waste streams. Thus, there is a need to develop greener recycling processes that make use of more environmentally friendly/benign lixivants (oxalic acid) to treat an LFP-rich BM that is contaminated by NMC or LCO chemistries.

This paper is a continuation of previous research [13], in which a range of different organic acids, namely, acetic, ascorbic, citric, malic, and oxalic acids, were screened for the selective leaching of a synthetic BM (a mixture of 95% LFP and 5% NMC). This research identified oxalic acid as a promising lixiviant for treating a mixed-chemistry black mass, as it could selectively leach the LFP material from the NMC material. The current paper evaluated whether the leaching conditions identified in [13] can be used to leach an industrially sourced, mixed-chemistry black mass and whether an organic acid can be used in a second-stage leach to recover the Cu, Co, Ni, and Mn left behind in the oxalic acid leach residue.

Much research has been conducted on the use of organic acids, such as ascorbic acid [14] and citric acid [15–17], synergistic combinations of acetic acid and ascorbic acid [18], and formic acid and acetic acid [19], to leach Ni, Co, and Mn from spent battery material. Similarly, during the screening experiments in Henderson et al.'s study [13], citric acid and ascorbic acid were identified as possible lixivants that could effectively leach NMC and LFP chemistries. Thus, given the high recoveries of Li and P (95.58% and 93.57%, respectively) in the first-stage oxalic acid leach, it is plausible that citric acid and ascorbic acid can be used to extract the remaining Ni, Co, and Mn from the leach residue. Another organic acid that was investigated for selective Cu, Co, Mn, and Ni extraction was glycine. The potential for glycine to extract Co and Ni was identified by Eksteen et al. [20], who determined that when leaching with a glycine-to-metal ratio of 8:1, pH 10, and 40% solids at room temperature for 672 h, approximately 76.3% and 83.5% of the Co and Ni could be extracted from a serpentine-rich sulfide ore. Subsequent research by the same research group [21,22] showed that the technology can be applied to diverse materials, such as nickeliferous pyrrhotite slimes and nickel-bearing cleaner tailings, and that leach times could be optimized down to 24 h. In another field of research, Li et al. [23] proved that Cu could be recovered from E-waste, namely, waste printed circuit boards (PCBs). This begs the question of whether glycine leaching can be used for treating spent LiBs. The

idea to use glycine for the recovery of Co from spent lithium-ion batteries is still relatively novel and was first reported in Chen et al.'s study [24]. Chen and coworkers [24] leached a LiCoO₂-rich black mass with a level of Ni, Mn, and Cu contamination. At the optimal conditions (300 g/L glycine, a solid-to-liquid ratio of 1:100, and 10% H₂O₂, at 80 °C for 3 h), Chen and coworkers [24] extracted 97.07%, 90.95%, 97.24%, 97.52%, and 90.21% of the Co, Li, Ni, Mn, and Cu, respectively. Given that an oxalic acid leach can selectively remove Li and P from the mixed chemistry black mass, there is, indeed, potential to use glycine to selectively recover any Cu, Ni, and Co that remains in the residue. Overall, the fundamental differences between the previous work [13] and this paper are that, firstly, an industrially sourced BM was leached. Therefore, the oxalic acid leaching system was tested on a more complex material that contained a mixture of different battery chemistries (LFP, LCO, NMC, etc.). Secondly, the current paper took the previous research further by identifying a second-stage leaching process capable of selectively extracting Co and Ni from the first-stage oxalic acid leach residue, which contained insoluble Co- and Ni-oxalates.

In conclusion, this paper evaluated whether the oxalic acid leaching stage developed in Henderson et al.'s study [13] can be applied to selectively leach LFP from an industrially sourced mixed-chemistry black mass that also contains NMC and LCO. If the first-stage oxalic acid leach proved successful, a second-stage leach using either citric acid, ascorbic acid, or glycine was investigated as a means to recover any remaining Cu, Co, Ni, and Mn from the leach residue, leaving behind a graphite-rich leach residue.

2. Method and Materials

2.1. Materials

The synthetic BM used in this research (second-stage leaching) comprised pristine LFP (Batch: 05323A4, Tucson, AZ, USA) and NMC 111 (Batch: 23922A7, Tucson, AZ, USA) purchased from MSE Suppliers. The industrially sourced BM was supplied by Envirostream (Laverton, Victoria, Australia), a subsidiary of Livium Australia, the composition of which is presented in Table 1 and Figure 1. The lixivants used in this research were oxalic acid dihydrate (C₂H₂O₄·2H₂O, ≥99.5%; batch: 428335; Chem-supply, Gillman, Australia), glycine (≥99 C₂H₅NO₂; G7126-1KG; Sigma-Aldrich, Saint Louis, MO, USA), sulfuric acid (98% H₂SO₄; Ajax Finechem Pty Ltd., Auckland, New Zealand), and ammonia (25% NH₃; batch: 2672; Rowe Scientific, Perth, Australia). When performing ICP, the following reagents were used: HNO₃ (70%; batch: 24070081; RCI Labscan Limited, Bangkok, Thailand), ICP phosphorus standard (1000 mg/L; High Purity Standards), and a multi-element standard (1000 mg/L; solution IV; Merck, Darmstadt, Germany).

Table 1. Industrial black mass composition obtained through XRF and ICP OES.

Al ₂ O ₃ (%)	C (%)	CaO (%)	Co (%)	Cu (%)	F (%)	Fe ₂ O ₃ (%)	K ₂ O (%)	Li (%)	MgO (%)	MnO (%)	Ni (%)	P ₂ O ₅ (%)	Pb (%)	SiO ₂ (%)	Sn (%)
13.35	32.10	0.11	1.50	4.50	2.55	15.40	0.05	1.52	0.06	0.50	4.31	13.15	0.06	1.84	0.09

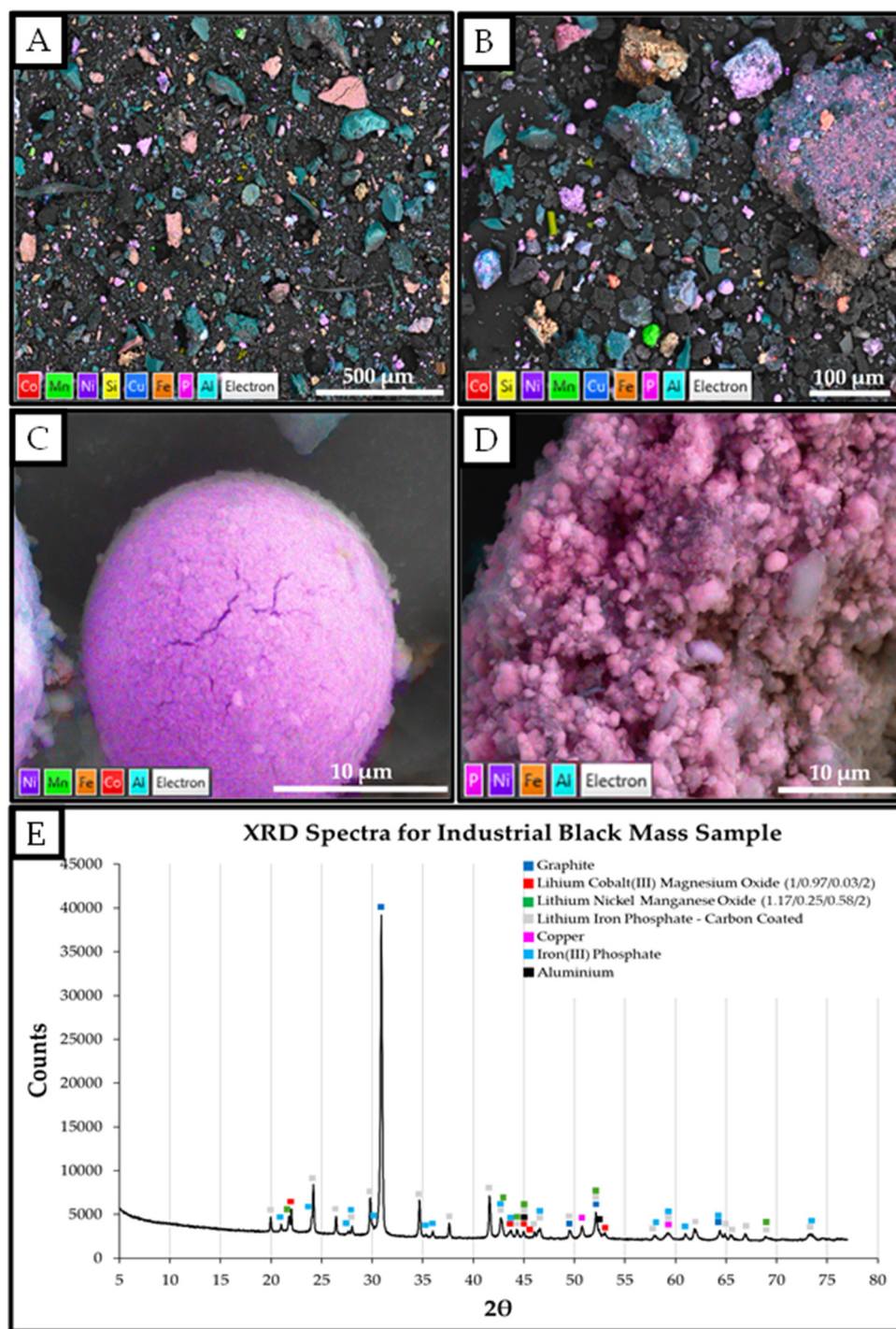


Figure 1. SEM-EDS of industrial black mass sample (A,B). SEM-EDS images of a Ni-, Co-, Mn-bearing particle (C) and LFP particle (D). XRD peaks of industrial black mass (E).

2.2. Method

2.2.1. Stage 1 Leaching—Oxalic Acid

Oxalic acid leaching tests were conducted using a typical bench-scale leaching set-up, namely, a three-necked round-bottom flask, connected to a water-cooled reflux condenser (to maintain the water balance), placed on a digital magnetic heating and stirring mantle (Across International, model: DigiM05, Bayswater, Australia). General leaching experiments were conducted at 2% solids, with 200 mL of oxalic acid and 4 g of the industrial black mass. Leaching parameters such as the temperature, solid-to-liquid ratio, acid concentration, and leaching time were varied, while the agitation rate was kept constant at

600 rpm. The pH, Eh, and temperature of the solutions were measured using a pH and Eh meter (model WP80DZ Rev 2.1, TPS, Brendale, Australia). The pH was monitored at the beginning and end of leaching, and no significant changes (less than ± 0.2) were observed (remained in the ideal pH range). Thus, there was no need to adjust the pH of the leaching system. Once leaching was complete, the solid and liquid were separated using vacuum filtration in a ceramic Büchner funnel and flask, using cellulose filter paper as the filter medium (MN 619 de; retention capacity: 1–2 μm ; 150 mm diameter; Macherey-Nagel, Düren, Germany), connected to a vacuum pump.

2.2.2. Stage 2 Leaching—Screening

The same procedure discussed above (see Section 2.2.1) was followed when conducting the second-stage leaching experiments. Initially, synthetic BM (95% pristine LFP and 5% pristine NMC) was leached using oxalic acid under conditions identified in Henderson et al.’s study [13] (1.25 M oxalic acid, pH 1.15, an agitation rate of 600 rpm, and 10% solids at 60 °C). The oxalate residue was then leached using citric acid (0.5 M), ascorbic acid (0.5 M), and glycine (30 g/L) with an agitation rate of 600 rpm and 2% solids at 60 °C for 2 h.

2.2.3. Stage 2 Leaching—Glycine

The glycine leaching system was partially optimized, following the same procedure in Section 2.2.1, by varying the leaching temperature (25, 40, and 60 °C) and glycine concentration (30, 45, 60, and 100 g/L), while parameters such as the leaching duration (2 h), agitation rate (600 rpm), and solid-to-liquid ratio (2%) were kept constant.

2.3. Analytical Techniques

2.3.1. Inductively Coupled Plasma–Optical Emission Spectroscopy (ICP-OES)

The identical ICP-OES method used to analyze the leaching solutions in Henderson et al.’s study [13] was followed. A Perkin Elmer Optical Emissions Spectrometer Optima 8300 (Perkin Elmer, Shelton, CT, USA), running Syngistix 3.0, was used to analyze all leaching solutions. Calibration standards were prepared using the P and multi-element standards stated in Section 2.1. Calibration standards of 1 ppm, 5 ppm, 10 ppm, 50 ppm, and 100 ppm were prepared using 5% HNO₃.

2.3.2. Scanning Electron Microscopy with Energy-Dispersive X-Ray Spectroscopy (SEM-EDS)

The pristine samples, reference samples, leach residues, and precipitates were analyzed using a Tescan Clara Field-Emission Scanning Microscope (FESEM, Tescan, Czech Republic) equipped with Oxford Instruments (Ultim Max 170 SDD X-ray detector) at the John de Laeter Centre (Curtin University). The SEM images were constructed by collecting secondary emissions (SEs) operating at beam currents between 100 and 300 pA, electron beam energies between 5 and 10 KeV, and a scanning rate between 1 and 5. The elemental analysis/chemical mapping was produced through the collection of electron backscatter diffraction data using the Oxford Instruments EBDS Symmetry Detector and then processing that data using the Oxford Instruments EDS software, namely, version 6.1 of Aztec Synergy.

2.3.3. XRD and XRF

As reported in Henderson et al.’s study [13], reference samples, leach residues, and precipitates were sent to ALS Metallurgy (Perth, Australia) for XRD and XRF analyses. When performing XRD, ALS Metallurgy followed the following procedure: The samples were packed into the sample holders and then analyzed using the Malvern Panalytical

Empyrean (Malvern Panalytical, Almelo, The Netherlands) equipped with a PIXcel1D X-ray detector. A cobalt X-ray tube was used during the analysis, which generated Co K α radiation with a wavelength of 1.789 Å, with an accelerating voltage of 40 kV and tube current of 40 mA. The data were collected for 118 s, over an angular range of 5–77° 2θ using a step size of 0.0121° 2θ. XRF samples were prepared as fused beads and analyzed using the Panalytical Axios unit. The analysis ranges for Al₂O₃, Co, Cu, Fe₂O₃, MnO, Ni, and P₂O₅ were <0.01–100 wt%, <0.001–7.34 wt%, <0.01–60 wt%, <0.01–100 wt%, <0.01–60 wt%, <0.01–25 wt%, and <0.01–15.6 wt%, respectively.

3. Results and Discussion

3.1. Black Mass Characterization

The BM used in this research was provided by Envirostream, a subsidiary of Livium Ltd. The BM composition was analyzed using XRF (Table 1), SEM-EDS (Figure 1A–D), and XRD (Figure 1E). The XRD analysis determined that the BM comprised both anodic and cathodic materials. The Al and graphite came from the anode, and Cu, LFP, and the Co-, Ni-, and Mn-bearing material came from the cathode (although there was some graphite associated with the cathode as well). The XRD findings, coupled with the XRF results, presented in Table 1, conclude that the industrial BM was LFP-rich with contaminants arising from the Co-, Mn-, and Ni-bearing battery chemistries. It was evident that there were large amounts of conductive foils present, namely, Cu (4.50%) and Al (Al₂O₃ = 13.35%), which correlated with approximately 7% Al. Figure 1A,B illustrate just how challenging working with BM is, as there is a range of different metals and materials. The large particle size ranges and diversity of shapes/morphologies imply that leaching efficiencies may differ even if the chemistry is similar to a pristine/synthetic black mass. The large amounts of foil contamination, both Al and Cu, visible in the SEM images, make downstream leaching processes more complex as they can be co-extracted along with target metals. This co-extraction results in decreased leaching efficiencies (higher reagent consumption) and requires additional purification steps for the removal of Al from Li and P, as well as Cu from Co and Ni from the respective leach solutions. Figure 1C,D are SEM-EDS images of a spherical Ni- and Co-rich particle (20 µm) and a larger, irregularly shaped LFP particle (around 200 µm). Overall, the XRD, XRF, and SEM-EDS results emphasize the complexity of an industrially sourced BM and, thus, the challenge associated with developing selective leaching processes.

3.2. Testing Synthetic BM Leaching Conditions on Industrial BM

The preceding work to this paper [13] investigated the leaching of a synthetic BM (LFP and NMC 111) using oxalic acid. The optimal leaching conditions for selectively targeting the LFP chemistry, from the synthetic BM, were identified to be 0.25 M oxalic acid, at room temperature, a natural pH of approximately 1.15, and 2% solids for an hour. Leaching under the aforementioned conditions resulted in the selective leaching of >93% of the Li and P, with minimal co-extractions of Fe (<13%), Mn (<9%), Co (0% (not detected)), and Ni (0% (not detected)). Thus, the optimal leaching conditions, identified in [13], were applied to the reference BM sample (see Section 3.1), and the leaching results are presented in Figure 2A–C.

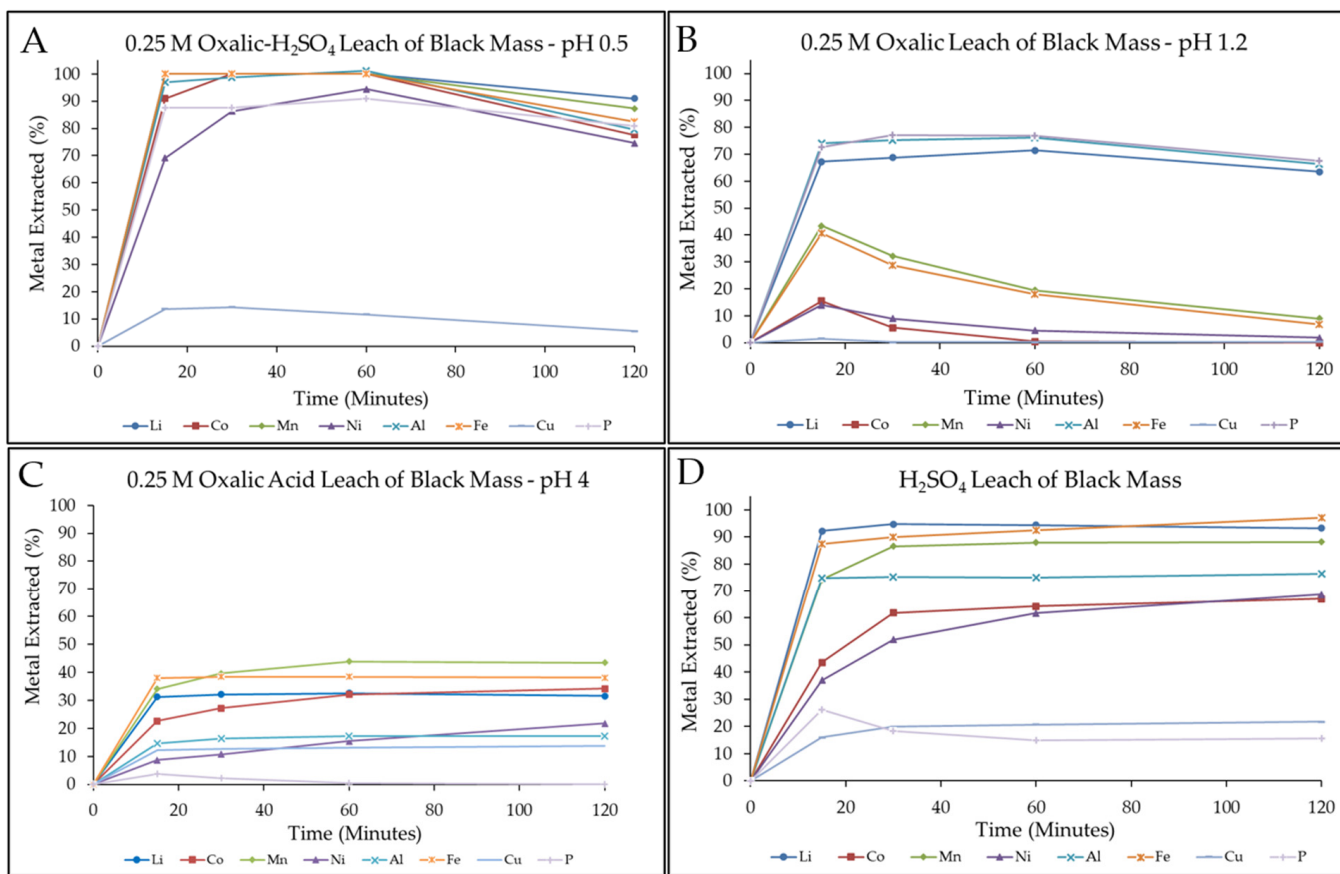


Figure 2. Three leaching experiments were conducted with 0.25 M oxalic acid, at room temperature, with an agitation speed of 600 rpm for 2 h, however, with varying pHs, namely, pH 0.5 (A), pH 1.2 (B), and pH 4 (C). A comparative H₂SO₄ leach was also conducted (D).

Researchers [25–27] have investigated the use of H₂SO₄ for the leaching of spent LIBs, as H₂SO₄ is a common lixiviant used throughout the battery recycling industry [2] due to its wide availability, ability to dissolve a range of different metals [15], and relatively low cost. As a reference, H₂SO₄ was used to leach the industrial BM, as presented in Figure 2D. The H₂SO₄ leach was conducted using the same volume of H₂SO₄ required to adjust the pH of the oxalic leaching system to pH 0.5. It is evident that when leaching with just H₂SO₄, the leaching was non-selective, with leaching efficiencies falling over a large range, from as low as 15% for P to as high as 97% for Fe. These results align with the observations of Henderson et al. [13].

Oxalic acid leaching at pH 0.5, as presented in Figure 2A, resulted in no selective metal dissolution. After 60 min, it was observed that approximately >98% of the Li, Co, Mn, Al, and Fe, 94% of the Ni, 90% of the P, and 11% of the Cu were extracted. However, these high extractions decreased with an increasing leaching duration. The initial increase was due to the initial dissolution rate of metals such as Co, Ni, Mn, and Fe being higher than the rate of oxalate complexation, allowing for the metal species to enter the leach solution [4].

Oxalic acid is capable of reducing metal species such as Co³⁺ and Mn⁴⁺ to Co²⁺ and Mn²⁺, allowing for their effective dissolution and later complexation with oxalate ions. The decrease in metal extraction with an increased leaching time aligns with [4] and can be attributed to the complexation of Fe²⁺, Mn²⁺, Co²⁺, and Ni²⁺ with C₂O₄²⁻, resulting in the formation of insoluble FeC₂O₄·2H₂O, MnC₂O₄·2H₂O, CoC₂O₄·2H₂O, and NiC₂O₄·2H₂O [17,28–30], all of which are presented in Table 2.

Table 2. Solubility and K_{sp} values for different metal–oxalates.

Metal–Oxalate Complex	K_{sp} Value	Solubility (g in 100 g of Water)	References
$\text{FeC}_2\text{O}_4 \cdot 2\text{H}_2\text{O}$	3.2×10^{-7}	Insoluble-0.078 ^a	
$\text{Fe}_2(\text{C}_2\text{O}_4)_3$	-	Soluble	
$\text{MnC}_2\text{O}_4 \cdot 2\text{H}_2\text{O}$	1.7×10^{-7}	Insoluble-0.032 ^b	
$\text{CoC}_2\text{O}_4 \cdot 2\text{H}_2\text{O}$	2.7×10^{-9}	Insoluble-0.0037 ^b	[4,17,28–32]
$\text{NiC}_2\text{O}_4 \cdot 2\text{H}_2\text{O}$	7.8×10^{-10}	Insoluble-0.0012 ^a	
$\text{CuC}_2\text{O}_4 \cdot 2\text{H}_2\text{O}$	4.43×10^{-10}	Insoluble-0.0026 ^b	
$\text{Al}_2(\text{C}_2\text{O}_4)_3 \cdot \text{H}_2\text{O}$	-	Insoluble	
$\text{Li}_2\text{C}_2\text{O}_4$		Soluble-5.87 ^a	

^a = 25 °C; ^b = 20 °C.

The leaching of BM using 0.25 M oxalic acid at pH 1.2, as presented in Figure 2B, resulted in the selective extraction of Al, Li, and P, namely, at 66.31%, 63.52%, and 67.65%, respectively, while only 6.84% of the Fe, 8.98% of the Mn, 1.77% of the Ni, 0% of the Co, and 0% of the Cu were co-extracted. The selectivity observed in Figure 2B is similar to the observations when leaching synthetic BM [13]. The greatest difference is the decreased Li and P leaching efficiencies when leaching the industrial BM. The Li and P extractions were roughly 30% higher in the synthetic leaching system, at 95.58% and 93.57%, respectively. The decrease in Li and P leaching efficiencies was a result of the high co-dissolution of Al; the dissolution of Al in an oxalate solution has previously been reported by [4,33]. The 0.25 M oxalic acid leaching solution had a pH of approximately 1.1–1.2 and an E_h of 560–590 mV. Thus, when constructing the species predominance diagrams in Figure 3A, it can be seen that under the tested leaching conditions, soluble $\text{Al}(\text{C}_2\text{O}_4)_2^-$ and $\text{Al}(\text{C}_2\text{O}_4)_3^-$ complexes were formed. No Cu was extracted as the reaction between Cu and oxalic acid resulted in the formation of an insoluble $\text{CuC}_2\text{O}_4 \cdot 2\text{H}_2\text{O}$ ($K_{sp} = 4.43 \times 10^{-10}$) [4,30]; this is illustrated in the predominance diagram presented in Figure 3B.

Finally, Figure 2C presents the findings of leaching the BM at pH 4. In the synthetic leaching system [13], it was concluded that adjusting the pH to 4 promoted the selective dissolution of Co, Ni, and Mn from the NMC 111 and LFP mixture. When applying the higher pH, the leaching conditions for the industrially sourced BM (Figure 1C) resulted in no distinctive shift in metal selectivity. However, at pHs above 4, an increase in Co, Ni, and Mn extraction was still observed (34.14%, 21.82%, and 43.40%, respectively). The increase was due to the increased likelihood of more soluble Co–, Ni–, and Mn–oxalate complexes forming at pHs above 4. Figure 3C–E present the species predominance diagrams for the Mn, Ni, and Co oxalate system. It is evident that soluble metal–oxalate complexes such as $\text{Co}(\text{C}_2\text{O}_4)_2^{2-}$, $\text{Ni}(\text{C}_2\text{O}_4)_2^{2-}$, and $\text{Mn}(\text{C}_2\text{O}_4)_2^{2-}$ became stable at high pHs. This finding is supported by the research of [34], who determined that the same soluble metal–oxalates as those identified in the predominance diagrams formed between pHs 4 and 5.

The levels of co-extracted Fe, Li, Al, and Cu were 38.10%, 31.52%, 17.35%, and 13.84%, respectively. The co-extraction of the aforementioned metals led to a decrease in available free oxalic acid, which, in turn, explained the decrease in the observed levels of Co, Ni, and Mn extracted. Researchers such as [35] determined that different NMC chemistries (e.g., 811, 622, 532, and 111) have varying leachabilities. Therefore, it was concluded that the higher the Ni content in a material, with the chloride leaching step, the more amenable to leaching the NMC material became. Meanwhile, the higher the Mn content, the more stable the NMC. Thus, the decrease in Co, Ni, and Mn extraction can be attributed to the mere fact that the industrial sample contained a variety of Mn-, Co-, and Ni-containing battery chemistries.

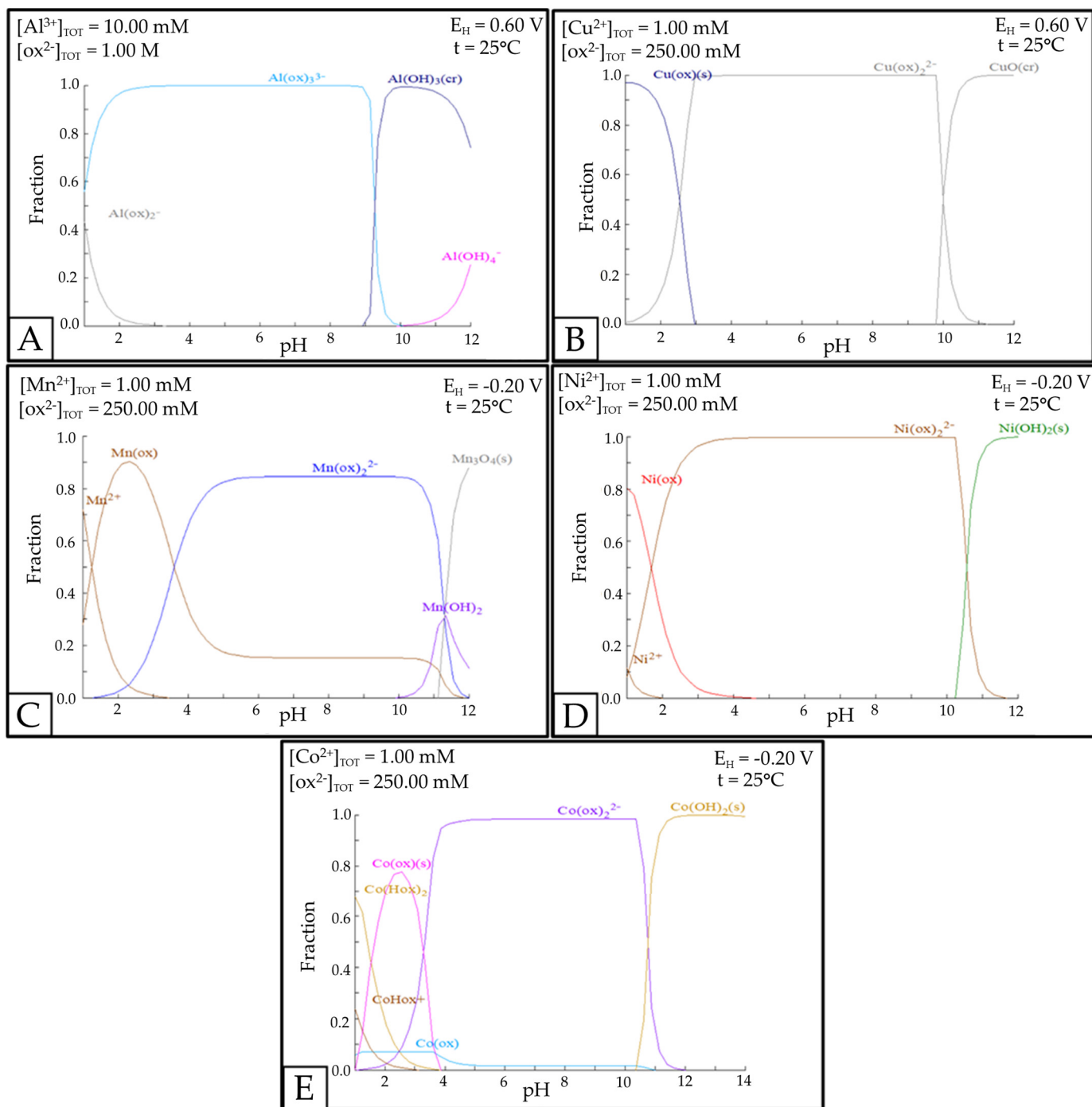


Figure 3. Species predominance diagrams of Al-oxalate (A), Cu-oxalate (B), Mn-oxalate (C), Ni-oxalate (D), and Co-oxalate (E) leaching systems (constructed using Medusa software (32-bit version)).

The XRF and XRD results (Table 1 and Figure 1E) support the above statement, as no clear NMC 111 chemistry was detected. Thus, considering the industrial BM sample contained a mixture of different variations of Ni-, Co-, and Mn-bearing chemistries, it is not unreasonable to suggest that the decreased selectivity was partly due to the different leachabilities of these materials.

The SEM images in Figure 4A–C illustrate the effect oxalic acid leaching had on the Ni-, Co-, and Mn-bearing particles (i.e., NMCs). Figure 4A,B present SEM images that illustrate how the surface of an NMC was affected post-oxalic leach. Post-leach, pitting was observed

on the particle surface, meaning the NMC was partially leached. However, there were also typical, cubic/block-like crystals on the surface of the NMC particle [1,28]. To determine the composition of the oxalate crystals, SEM-EDS was performed. The results are presented in Figure 4C. The crystals on the surface were determined to be mainly Fe and O, meaning that the Fe–oxalate likely precipitated onto the NMC particles’ surfaces. Thus, this prevented the complete dissolution of the NMC into single Co–, Ni–, and Mn–oxalate crystals. The above findings are supported by [5], in which Saleem and coworkers observed that the leaching of NMC particles could be inhibited by an Fe–oxalate layer, which precipitated onto the NMC particles.

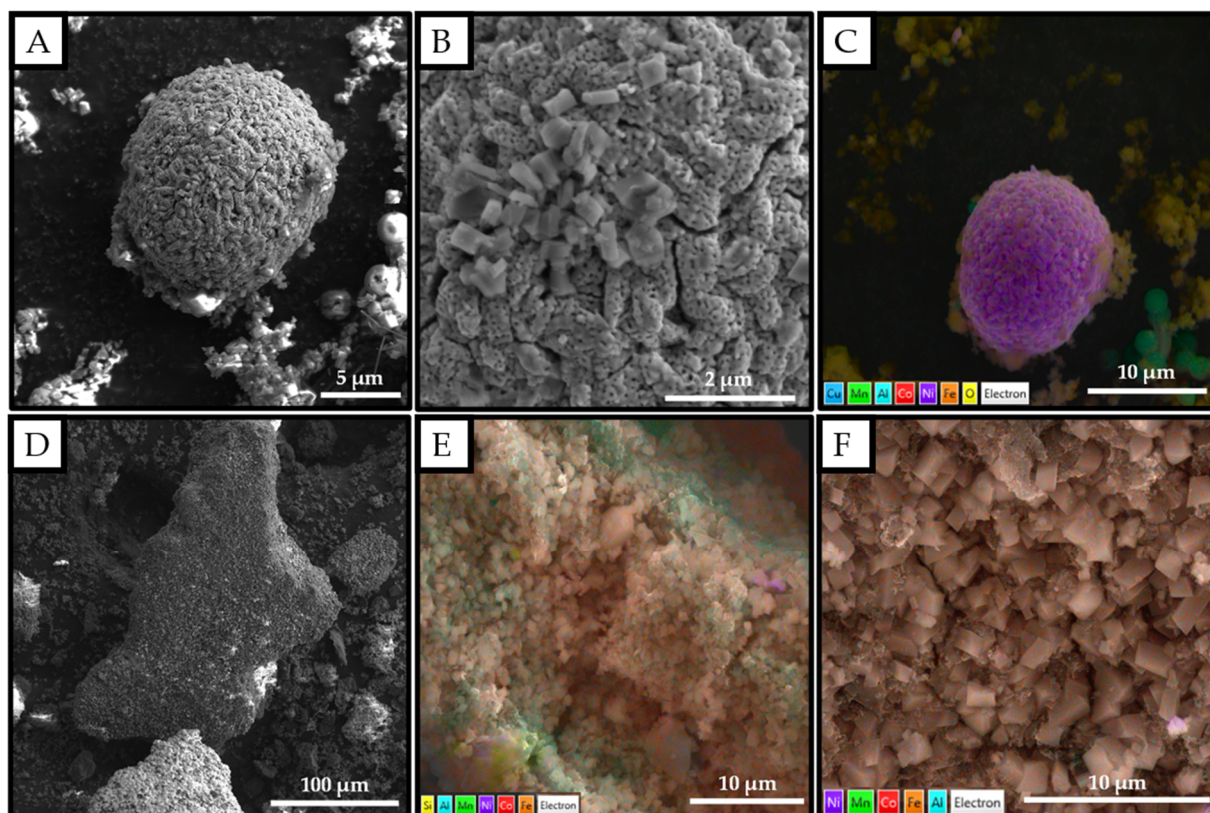


Figure 4. SEM images of an oxalic acid-leached NMC particle (**A,B**) and the EDS chemical map of the NMC particle (**C**). SEM image of an oxalic acid-leached LFP particle (**D**), along with a close-up SEM-EDS chemical map of the leached LFP particles (**E,F**).

The SEM and SEM-EDS images presented in Figure 4D,E are those of an LFP particle post-oxalic leach. The findings align well with those observed in the synthetic leaching system [13], as the same distinctive cubic oxalate crystals were present. This confirms that the LFP was leached, and what remained were insoluble Fe–oxalate crystals. In the SEM-EDS image (see Figure 4F), a Ni–oxalate crystal was also observed on the LFP surface (a purple crystal).

Overall, the optimal leaching conditions identified for leaching the synthetic BM were successfully applied to an industrially sourced mixed-chemistry BM. The low- (pH 0.5) and natural-pH (pH 1.1–1.2) leaches align strongly with the results presented in [13]. The advantage of leaching at pH 1.1–1.2 is that Al, Li, and P can be selectively removed from a mixed-chemistry BM, leaving behind a C-, Ni-, Co-, Cu-, Mn-, and Fe-rich leach residue. However, the leaching parameters need to be optimized to ensure that >90% of the Li and P can be selectively extracted from the industrial BM.

3.3. Optimizing Leaching Parameters—Oxalic Acid Leaching of Industrial BM

3.3.1. Changing Concentration

Leaching the industrially sourced BM using 0.25 M oxalic acid, at room temperature, with 2% solids and an agitation rate of 600 rpm for 2 h (see Figure 5A) resulted in insufficient Li and P extractions (<80%). Thus, higher oxalic acid concentrations were investigated to determine whether the Li and P extractions could be increased. Figure 5B,C present the data for the 0.5 M and 1 M oxalic acid leaches. Initially, when increasing the acid concentration from 0.25 to 0.5 M, it was observed that the extraction of Li and P increased significantly, from 63.52% and 67.65% to 92.22% and 88.65%, respectively. The extraction of Al was observed to have slightly increased, from 66.31% to 69.19%. Thus, it can be concluded that when leaching with 0.25 M, oxalic acid was the limiting reagent, as Al was co-extracted. Therefore, higher oxalic acid concentrations were required to account for the high co-extraction of Al (69%), ensuring adequate Li and P extractions. As the concentration was increased to 1 M (see Figure 5D), an increase, approximately 6%, in the extraction of Li and P was observed, leading to final Li and P extractions of 98.95% and 94.76%, respectively.

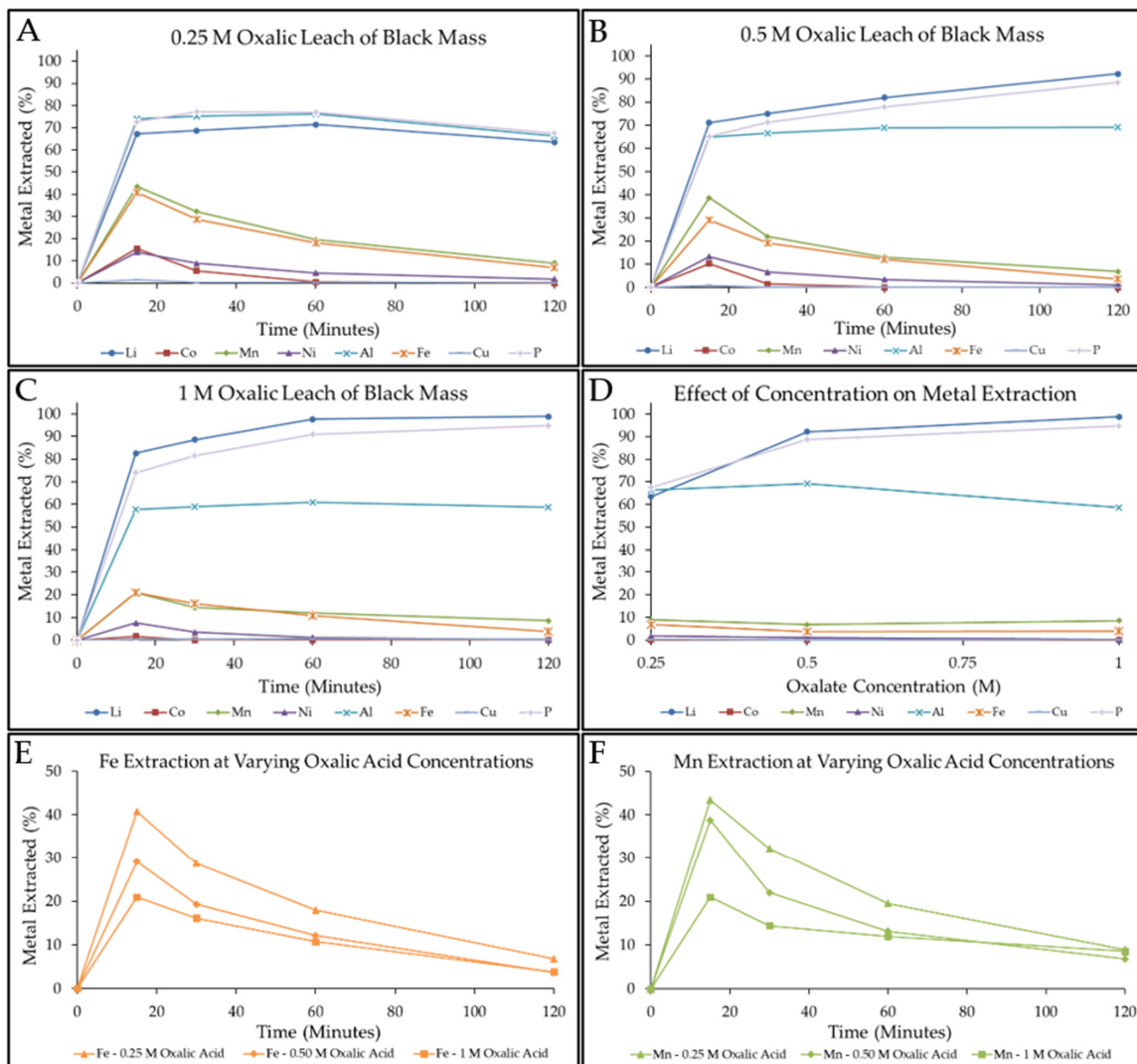


Figure 5. All oxalic acid leaching systems were conducted at room temperature, with 2% solids and an agitation speed of 600 rpm for 2 h with varying oxalic acid concentrations, namely, 0.25 M (A), 0.50 M (B), and 1 M (C). The effect of a changing concentration on metal extraction after leaching for 2 h (D). The effects of time and acid concentration on the extraction of Fe (E) and Mn (F).

The greatest advantage of operating at high oxalic acid concentrations was observed when investigating the co-extraction of Co, Ni, Mn, and Fe. Figure 5A–C illustrate that at 15 min, a large spike in the co-extraction of Co, Ni, Mn, and Fe was observed, followed by a decrease in metal extraction with an increased leaching time. Figure 5E,F emphasize that as the oxalic acid concentration and leaching time were increased, the co-extractions of metals such as Fe and Mn decreased. As mentioned previously, this was due to the respective metals having enough time to form insoluble metal–oxalates (Fe(II)–, Co–, and Ni–oxalates). The decrease in metal co-extraction, coupled with the higher Li and P extractions at higher oxalic acid concentrations, means that when designing an industrial oxalic acid process, slightly elevated concentrations should be favoured to promote adequate leaching with a high degree of selectivity. However, as seen in the paper-manufacturing industry, oxalic acid can cause scaling [36]. Thus, one should be careful not to increase the oxalic acid concentration too much, as solubility becomes an issue. This would require elevated temperatures to prevent metal–oxalates from precipitating out of solution, lowering leaching efficiencies and causing scaling of reaction vessels. Consequently, a 0.5 M oxalic acid concentration was chosen, as it allows for the use of slightly higher solid-to-liquid ratios, all while being able to extract >92% and >88% of the Li and P, respectively.

3.3.2. Changing Temperature

The temperature of the oxalic acid leaching system was varied between 25 °C and 60 °C, while parameters such as the agitation speed (600 rpm), leaching time (2 h), solid-to-liquid ratio (2%), and acid concentration were kept constant (0.5 M). Initially, after 15 min, as the temperature increased from 25 °C (Figure 6A) to 40 °C (Figure 6B), there was an increase in Li extraction from 74.71% to 81.61% which then increased to 83.8% at 60 °C. It was observed that the Al and P extractions were similar to that of Li, namely, exhibiting a minimal increase in metal extraction with an increase in temperature. Overall, after 2 h, the differences in the leaching efficiencies for Al, Li, and P (see Figure 5D) were not significant as they differed by 2–5% which was within the calculated standard deviations for the oxalic leaching system.

Meanwhile, the co-extraction of Fe, Ni, Mn, and Co was highly sensitive to changes in temperature. Initially, after 15 min, an increase in temperature resulted in a decrease in the amount of Co, Ni, Mn, and Fe being co-extracted. The decrease in the initial extraction was due to an increase in the rate at which insoluble metal–oxalates were formed. The increase in temperature resulted in more oxalic ions being released into solution, leading to a higher rate of complexation between the dissolved metal species and oxalate ions. Thus, the Fe–, Co–, Ni–, and Mn–oxalates precipitated from the solution [29] (see Table 2). When looking at Co and Ni, it was evident that longer leaching times allowed for the formation of insoluble Ni– and Co–oxalates. Therefore, any Co and Ni that initially dissolved precipitated out of solution with an increased leaching time. The decreasing trend observed above was observed for Mn and Fe; this, too, was attributed to the formation of insoluble Fe– and Mn–oxalates. However, Fe can be present as either Fe^{2+} or Fe^{3+} , of which $\text{Fe}(\text{III})$ –oxalate is more soluble than the insoluble $\text{Fe}(\text{II})$ –oxalate. Regardless of the leaching temperature, the co-extraction of Fe remained relatively constant, between 5 and 9%.

The final Mn extraction, after 2 h, was most significantly affected by changes in temperature. When operating at room temperature, the Mn in solution was approximately 9% and then significantly increased to 24%. This was due to the increase in the solubility of Mn–oxalate at elevated temperatures. It is well established that the solubility of metal complexes generally increases with increased solution temperatures.

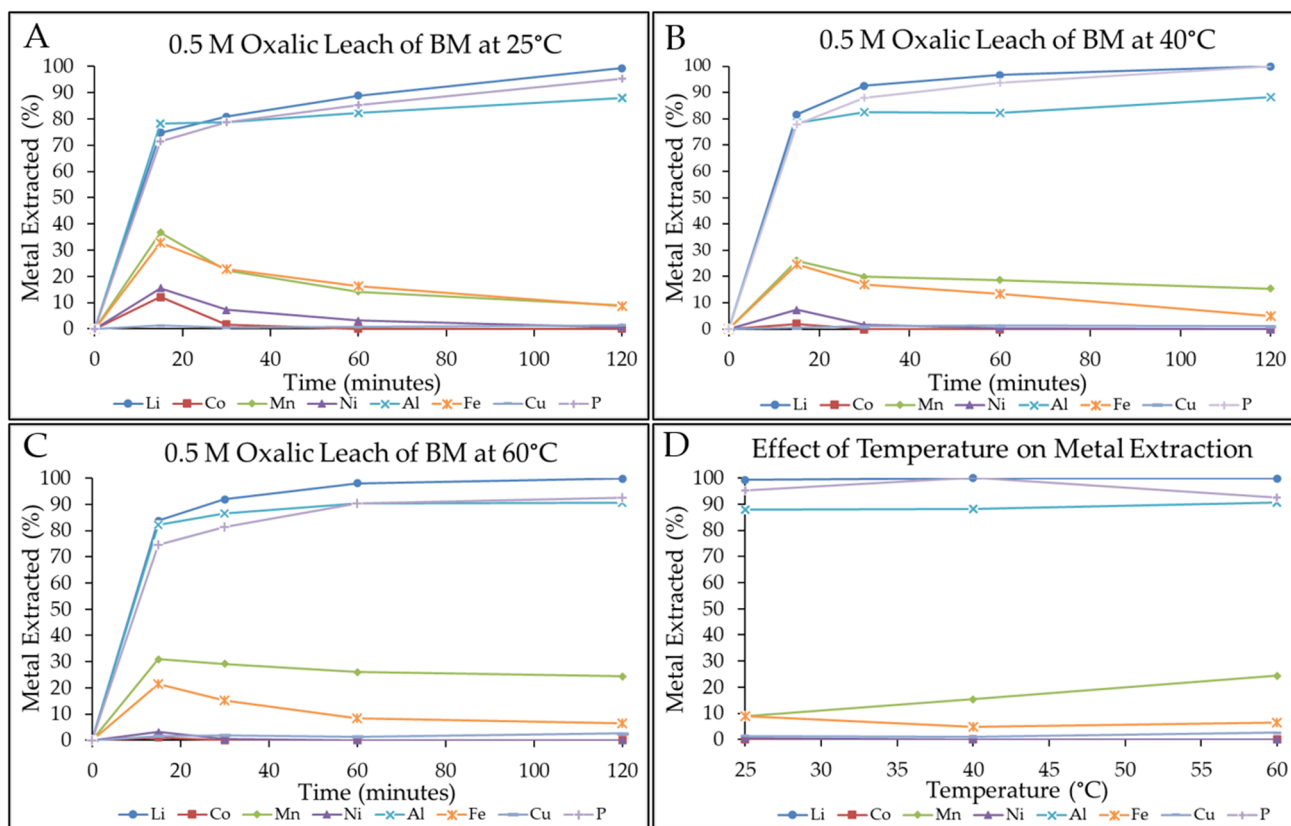


Figure 6. The effect of temperature on leaching efficiency. Leaching was conducted at 2% solids for 2 h, at agitation speeds of 600 rpm and 0.5 M, with varying temperatures, namely, 25 °C (A), 40 °C (B), and 60 °C (C). The effect of changing temperature on metal extractions after a 2 h leach (D).

Finally, the Cu foil was only slightly leached (<2%) by oxalic acid, and any Cu that was dissolved was later complexed with oxalic acid and precipitated out as an insoluble Cu–oxalate (with a low solubility of 0.0026 g in 100 g of H₂O at 20 °C) [30].

3.3.3. Changing Solid-to-Liquid Ratio

The initial leaching experiments were conducted at 2% solids. For the leaching process to be industrially applicable, it should be able to operate at higher solid-to-liquid ratios (e.g., 10% or larger). To ensure comparability between the different solid-to-liquid ratio experiments, the oxalic acid-to-metal ratio was kept constant. Thus, oxalic acid concentrations of 0.5 M, 1.25 M, and 2.5 M were required when operating at 2%, 5%, and 10% solids, respectively. The maximum solubility of oxalic acid, at room temperature, is approximately 108 g/L (1.2 M) [37]. Therefore, the leaching temperature needs to be increased when using higher oxalic acid concentrations; for that reason, leaching was conducted at 60 °C, ensuring full oxalic acid dissolution when working with both the 1.25 M and 2.5 M solutions.

The results, presented in Figure 7A–C, illustrated that as the solid-to-liquid ratio increased, so did the selectivity of the oxalic leaching system. When increasing the solid-to-liquid ratio from 2% to 5% solids, the extractions of Al, Li, and P, after 15 min, increased from 82.23%, 83.80%, and 74.70% to 86.38%, 93.96%, and 86.09%, respectively. At 10% solids, the extracted Li and P increased further to 100% and 96.47%, respectively. While Al was observed to increase slightly to 87.56%. Overall, the Li and P extractions increased significantly as the solid-to-liquid ratio increased; however, only slight increases in Al extraction were observed.

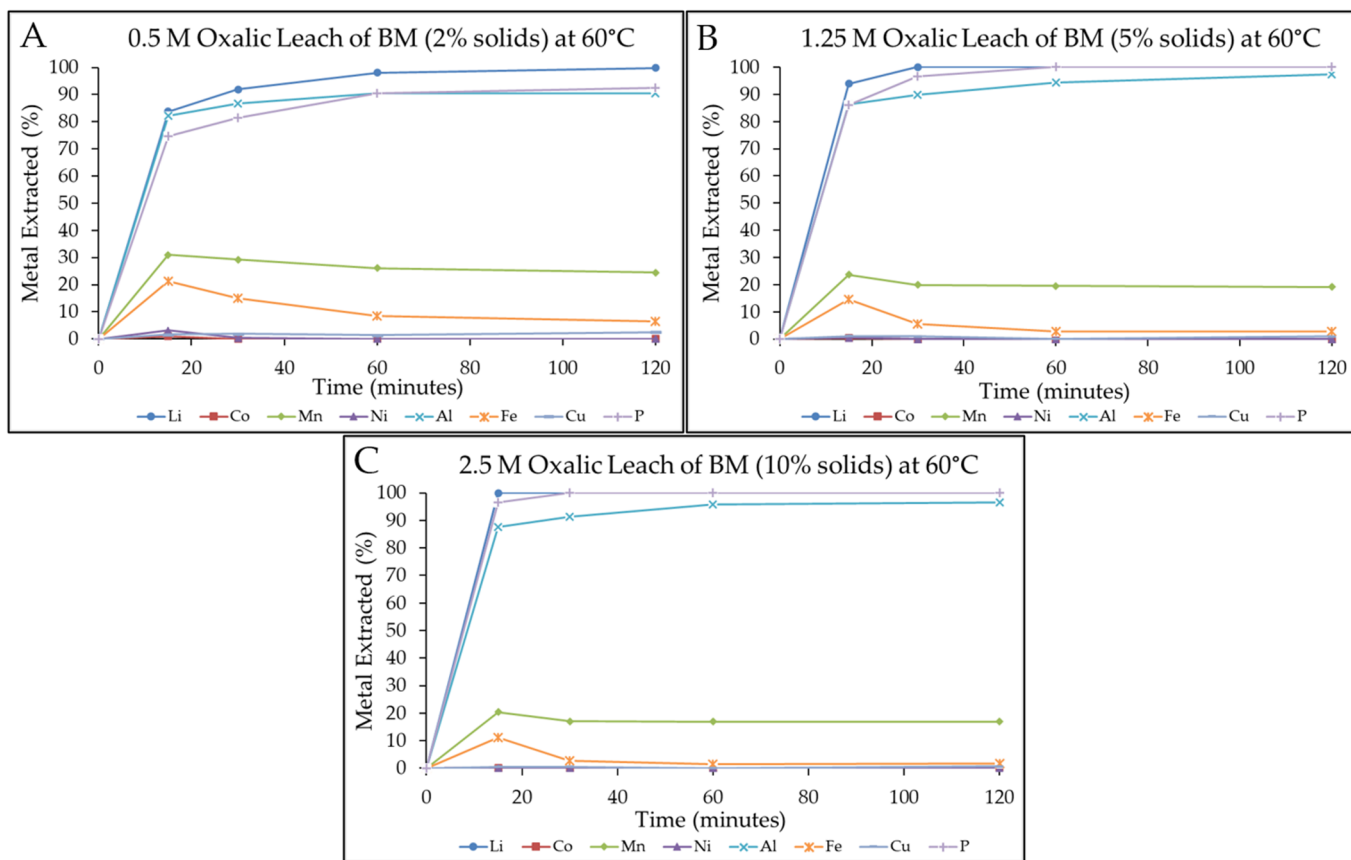


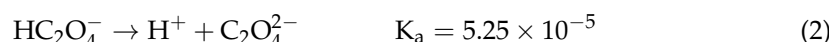
Figure 7. Effect of a changing solid-to-liquid ratio on metal extraction. The molar ratio of oxalic acid to metals was kept constant along with the leaching temperature ($60\text{ }^{\circ}\text{C}$), agitation speed (600 rpm), and leaching time (2 h), with variations in the solid-to-liquid ratios, namely, 2% (A), 5% (B), and 10% (C).

The co-extraction of Fe, Co, Cu, Ni, and Mn was observed to have the opposite trend to that of Li, Al, and P. As the solid-to-liquid ratio increased, the co-extraction of Mn, Fe, Cu, Co, and Ni decreased (at 2% solids after 2 h) from 24.44%, 6.58%, 2.54%, 0%, and 0% to 16.89%, 1.80%, 0.70%, 0.26%, and 0%, respectively. When operating at higher solid-to-liquid ratios, more BM was required as well as higher concentrations of oxalic acid, leading to a higher concentration of the metal species and oxalate ions in the same unit volume. Thus, there was an increased likelihood for interaction between the metal species and oxalate ions, increasing the rate at which insoluble complexes formed. When leaching for 2 h, at $60\text{ }^{\circ}\text{C}$, the selectivity of the oxalic acid leaching of the mixed-chemistry black mass increased with an increasing solid-to-liquid ratio. However, as previously mentioned, high oxalic acid concentrations (e.g., $>1.2\text{ M}$) can be challenging at an industrial scale as alkaline earth oxalates can form, leading to scaling of equipment and lowered metal extraction rates. Thus, it is recommended that, at most, 5% solids can be leached using this system, as it achieved $>97\%$ extraction of the Al, Li, and P while extracting $<19.11\%$, 2.75% , 0.94% , 0% , and 0% of the Mn, Fe, Cu, Co, and Ni.

3.3.4. Oxalic Acid Consumption and Possible Reactions

It is important to understand the consumption of oxalic acid during the leaching of industrially sourced BM. To determine acid consumption, ion chromatography was utilized to measure the concentration of $\text{C}_2\text{O}_4^{2-}$ in the solution. Figure 8 presents the data for a 0.5 M oxalic leaching system. Overlaid in red is the concentration of $\text{C}_2\text{O}_4^{2-}$ in the solution. Initially, the leaching solution contained 63.36 g/L of oxalic acid; however,

Figure 8 only reported that 33 g/L was present. This was due to the partial dissolution of oxalic acid in the solution. As oxalic acid is a diprotic acid, it can donate two H^+ ions. The dissociation of oxalic acid occurs in two steps, the first of which occurs at pH 1.23, in which the first H^+ ion is donated (Equation (1)), and the second at pH 4.19, where all of the H^+ ions are donated (Equation (2)) [8,29]. In reality, the diprotic acids can partially dissociate over a pH range, explaining why the initial content of the $\text{C}_2\text{O}_4^{2-}$ anion was not 63.36 g/L, as it had not completely dissociated. The dissociation equations below were presented by [29].



The concentration of $\text{C}_2\text{O}_4^{2-}$ initially decreased as metal oxalates formed. It is evident that as the concentration of Mn, Fe, Co, and Ni in the solution decreased, the concentration of $\text{C}_2\text{O}_4^{2-}$ in the solution increased. This can be explained through Le Chatelier's principle, as, initially, the free $\text{C}_2\text{O}_4^{2-}$ was consumed during the formation of complexes with the metal ions in the solution. Both soluble and insoluble metal–oxalates were formed. In this case, the Fe(II)–, Co–, and Ni–oxalates were insoluble, while the Fe(III)– and Mn–oxalates were soluble/partially soluble. Thus, with time, the different insoluble metal–oxalates precipitated out of the solution, leading to a decrease in the overall concentration of free $\text{C}_2\text{O}_4^{2-}$ ions. This caused a shift in the equilibrium, which then favored the dissolution of additional oxalic acid to replace the oxalate ions lost through precipitation.

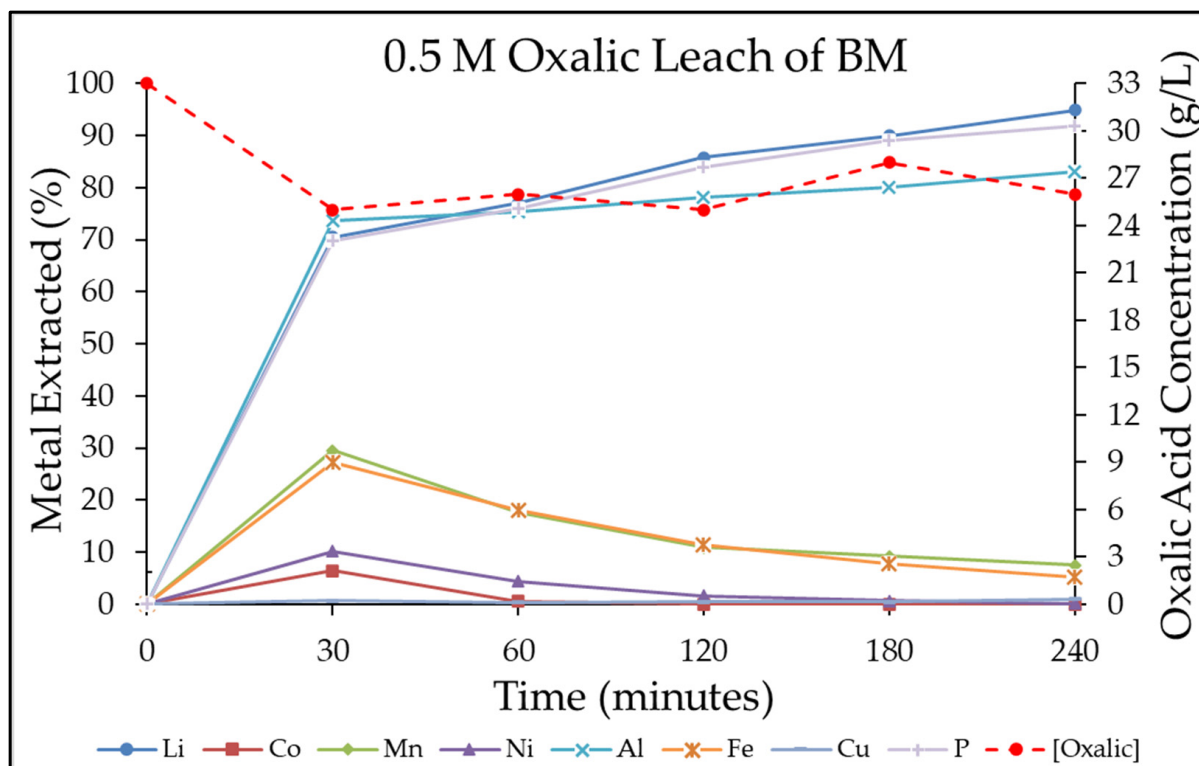
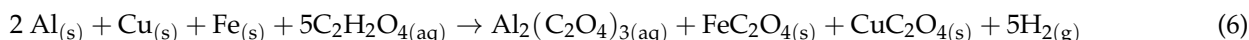
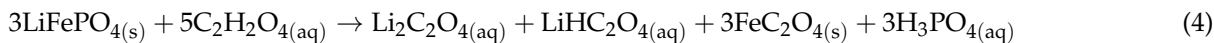
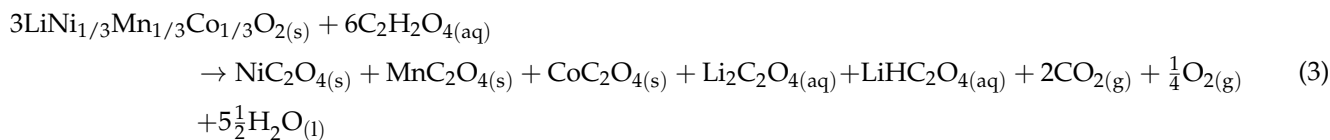


Figure 8. Tracking oxalic acid concentration during the leaching of black mass (0.5 M oxalic acid, 2% solids, 600 rpm, and room temperature for 4 h).

Numerous researchers have proposed reactions of battery materials with oxalic acid [1,3,4,6,8,13,28,38]. Equations (3)–(6) describe the leaching of a mixed-chemistry black mass, as understood in this research. The complete verification of the individual reaction steps is beyond the scope of the research reported here. The BM contained a range of

different Ni-, Co-, and Mn-bearing battery chemistries, and, thus, for the sake of demonstrating the principles, it was assumed that the BM comprised a mixture of NMC 111, LCO, and LFP. The reactions between the different battery chemistries and oxalic are presented in Equations (3)–(5), while the reaction between the metal foils and possible Fe casing is described in Equation (6). In reality, the ratio of Ni, Mn, and Co varied randomly depending on the material treated on a given day, given that a typical recycling plant would treat a highly variable feed when it processes end-of-life LiBs (rather than production scrap, which is more consistent). The equations are fairly generic battery leaching equations and assume that only certain oxalate species are generated; however, in reality, there is a range of different species that can form, depending on the leaching conditions used (i.e., $\text{Al}(\text{C}_2\text{O}_4)_2^-$ and $\text{Al}(\text{C}_2\text{O}_4)_3^{3-}$ [33]). The presence of CO_2 is due to the ability of oxalate to reduce Co^{3+} and Mn^{4+} to Co^{2+} and Mn^{2+} [28]; this process results in the production of CO_2 [8]. In the industrially sourced BM, there were metal foils (Al and Cu) as well as metallic Fe from the battery casing. Thus, it is important to emphasize that these, too, were leached. Equation (6) presents the leaching reactions for these metals [4]. The reactions presented illustrate that H_2 is produced, and, thus, if large amounts of Al, Cu, and Fe are in the feedstock, one should implement adequate measures to safely deal with the presence of H_2 , as this could lead to unexpected explosions if produced in large amounts.



3.4. Second-Stage Leaching—Screening Lixiviants in Synthetic Black Mass

The initial screening tests conducted in [13], on a synthetic material, BM, identified lixivants capable of dissolving impurities such as Co, Ni, and Mn. In the initial work, pristine synthetic BM was leached using ascorbic and citric acid. Ascorbic acid leached high levels of Ni, Co, Mn, and P. In theory, if the Li and P were removed, the leaching system could selectively remove >70% of the Mn and >90% of the Co and Ni (see Figure 1A in [13]). Similarly, citric acid was shown to be able to leach >70% of all the Fe, Ni, Mn, and Co. Consequently, both ascorbic and citric acid were investigated for the leaching of the black mass residue post-oxalic acid leach.

Figure 9A presents the metal extraction results for the oxalic leaching of synthetic BM (95% LFP and 5% NMC 111). The leaching was conducted using parameters identified in previous work, namely, 1.25 M oxalic acid, at 60 °C, with an agitation rate of 600 rpm and 10% solids for 60 min. The findings concluded that approximately 100% of the Li and P was extracted, while only 11% of the Fe was co-extracted. The oxalic acid leach residue, rich in C, Co, Ni, Mn, and Fe, was then leached in a second-stage leach using 0.5 M ascorbic acid (see Figure 9B) and citric acid (see Figure 9C). It was observed that, under the conditions identified for the synthetic leach systems, poor metal dissolution efficiencies were achieved when leaching the residue. The citric acid leach performed best, achieving leaching efficiencies of 18.66%, 12.37%, and 0.19% for Fe, Mn, and Co, respectively, whereas the ascorbic leaching system only dissolved 2.13% and 1.85% of the Mn and Fe, respectively. In both cases, the poor extraction of Co, Ni, Mn, and Fe can be attributed to the presence of these metals as metal-oxalates in the residue. It is well established that Co-, Ni-, Fe-, and

Mn–oxalates are highly insoluble in acidic, aqueous systems. Thus, when leached in citric and ascorbic acid systems, these lixivants are not sufficient to break the strong lattice bonds formed between the metal–oxalates. This is supported by research conducted by [17,39,40], which discussed the leaching of spent battery materials using ascorbic and citric acid. Metal ions (Co, Ni, and Mn) were subsequently recovered from the respective leach solutions using oxalic acid, implying that the Co–, Ni–, and Mn–oxalate complexes were more stable than the citrate– and ascorbic acid–metal complexes. The stability of metal–oxalates makes them less amenable to leaching. This is further supported by [40], who stated that complexes such as Co–citrate are weak, allowing for precipitation as Co(II)–oxalate.

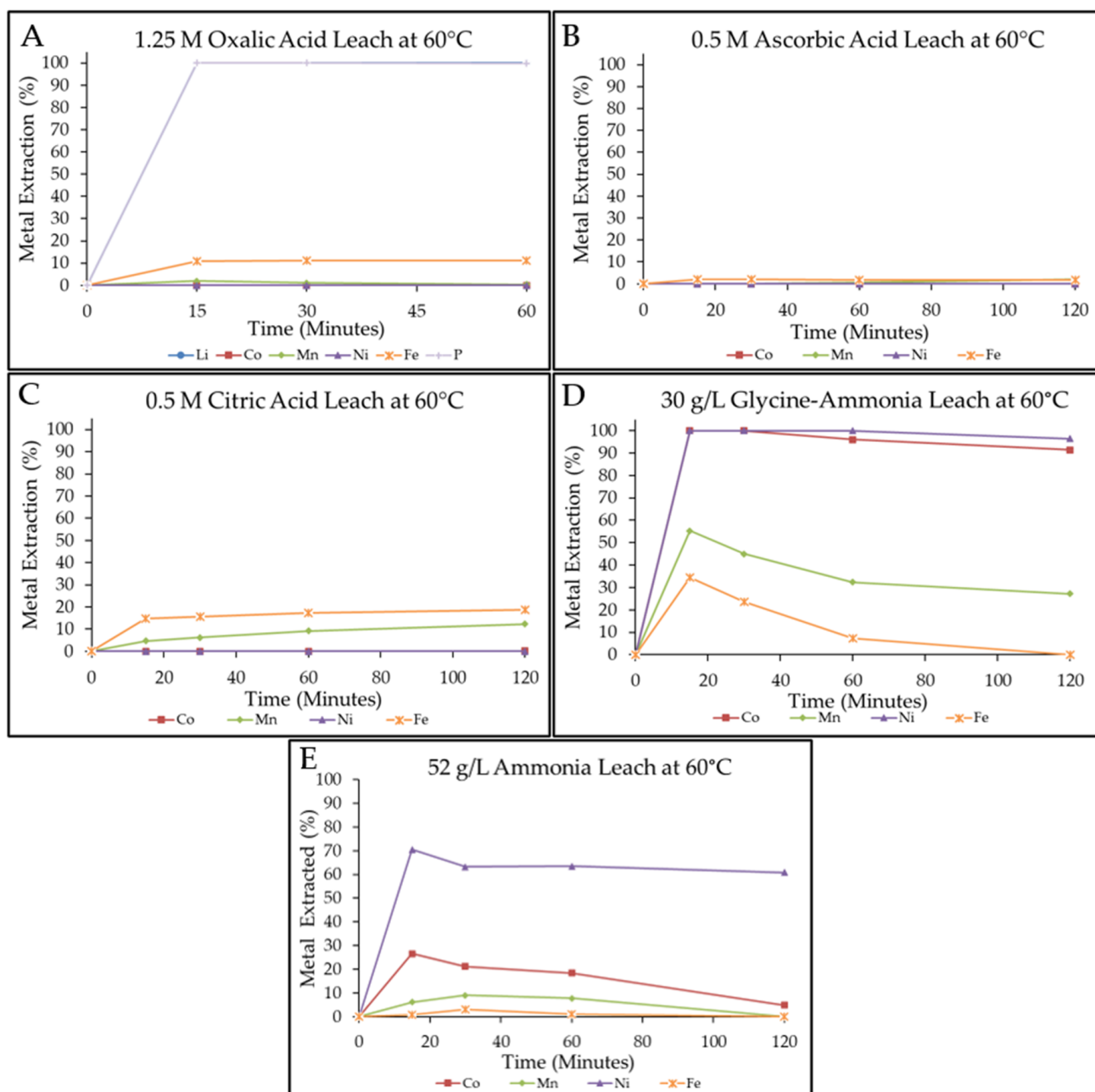


Figure 9. First-stage oxalic acid leach of synthetic black mass (1.25 M, 60 °C, 600 rpm, and 10% solids for 1 h) (A); second-stage screening leaching of first-stage leaching residue (60 °C, 600 rpm, and 2% solids for 2 h), using 0.5 M ascorbic acid (B), 0.5 M citric acid (C), and 30 g/L of glycine (D). Reference ammonia leach (E).

In previous studies, it was determined that Co-, Ni-, and Mn-oxalates are more soluble at higher pHs. Many researchers identified glycine as a lixiviant of choice for the selective leaching of Cu, Co, and Ni from waste PCBs [23,41,42], ore bodies [20,21], and, most recently, from spent LiBs [24,43]. Glycine leaching of Co and Ni requires an alkaline environment, and thus, considering that metal-oxalates become more soluble at higher pHs, the glycine leaching system was investigated for the selective leaching of the oxalic acid leach residue.

Figure 9D presents the metal extraction results for a glycine–ammonia leach. The leaching was conducted using 30 g/L of glycine and ammonia to adjust the pH to around 9/10 and an agitation speed of 600 rpm for 2 h at 60 °C. It was concluded that (see Figure 9D) 100% of the Co and Ni, 55.29% of the Mn, and 34.49% of the Fe were extracted in just 15 min. The initial pH of the above glycine leaching solution was approximately 9.9, and after leaching, it decreased to 9.4. Inspecting the Pourbaix/Eh–pH diagrams presented in Figure 10A–D illustrates that Co, Ni, and Mn formed soluble metal–glycinates complexes, whereas Fe and Mn formed insoluble metal oxides/hydroxides at these pHs. The predicted formation of insoluble compounds, such as Fe hydroxides (i.e., Fe(OH)_3) (see Table 3)) [44,45] or Fe oxides (i.e., Fe_2O_3 and Fe_3O_4) [20,23], explains why dissolved iron decreased with time as it precipitated out of solution. The Mn was dissolved as Mn–glycinate; however, as the glycine was consumed, there was insufficient free glycine left to form stable Mn–glycinate. This allowed for the formation of insoluble Mn oxides and Mn hydroxide, which precipitated out of solution. The above findings are promising as they illustrate that glycine leaching can be used to selectively remove Co and Ni from the oxalate leach residue. Table 3 presents the formation constants for the various metal–glycinates as well as the K_{sp} of the respective metal hydroxides.

Table 3. Formation constants of various metal–glycinates and K_{sp} values of the respective metal hydroxides.

Metals Cations	Formation Constants (β) ($I = 0 \text{ mol dm}^{-3}$; Temp. = 25)	Reference
Mn(II)	$\beta_1 = 1.51 \times 10^3$; $\beta_2 = 2.95 \times 10^5$	[46]
Fe(II)	$\beta_1 = 4.90 \times 10^3$; $\beta_2 = 1.20 \times 10^5$	[47]
Co(II)	$\beta_1 = 1.10 \times 10^5$; $\beta_2 = 1.45 \times 10^9$; $\beta_3 = 3.80 \times 10^{11}$	[46]
Ni(II)	$\beta_1 = 1.45 \times 10^6$; $\beta_2 = 1.29 \times 10^{11}$; $\beta_3 = 2.69 \times 10^{14}$	[48]
Cu(II)	$\beta_1 = 3.31 \times 10^8$; $\beta_2 = 5.62 \times 10^{15}$	[48]
Metal Hydroxides	K_{sp} Values	Reference
Mn(OH)_2	2×10^{-13}	
Co(OH)_2	1.58×10^{-15}	
Ni(OH)_2	2×10^{-15}	
Fe(OH)_2	7.94×10^{-16}	[49]
Cu(OH)_2	2.51×10^{-19}	
Fe(OH)_3	3.98×10^{-38}	
Co(OH)_3	5.01×10^{-45}	

The results in Figure 9E illustrate that when leaching with just ammonia, Ni was extracted. However, the leaching system was not capable of leaching all three target metals, namely, Co, Ni, and Mn. Thus, the glycine (pH adjustments with ammonia) leaching system was the best approach tested to selectively recover Co, Ni, and Mn. Maintaining ammonia concentrations at elevated temperatures is problematic due to its vapor pressure.

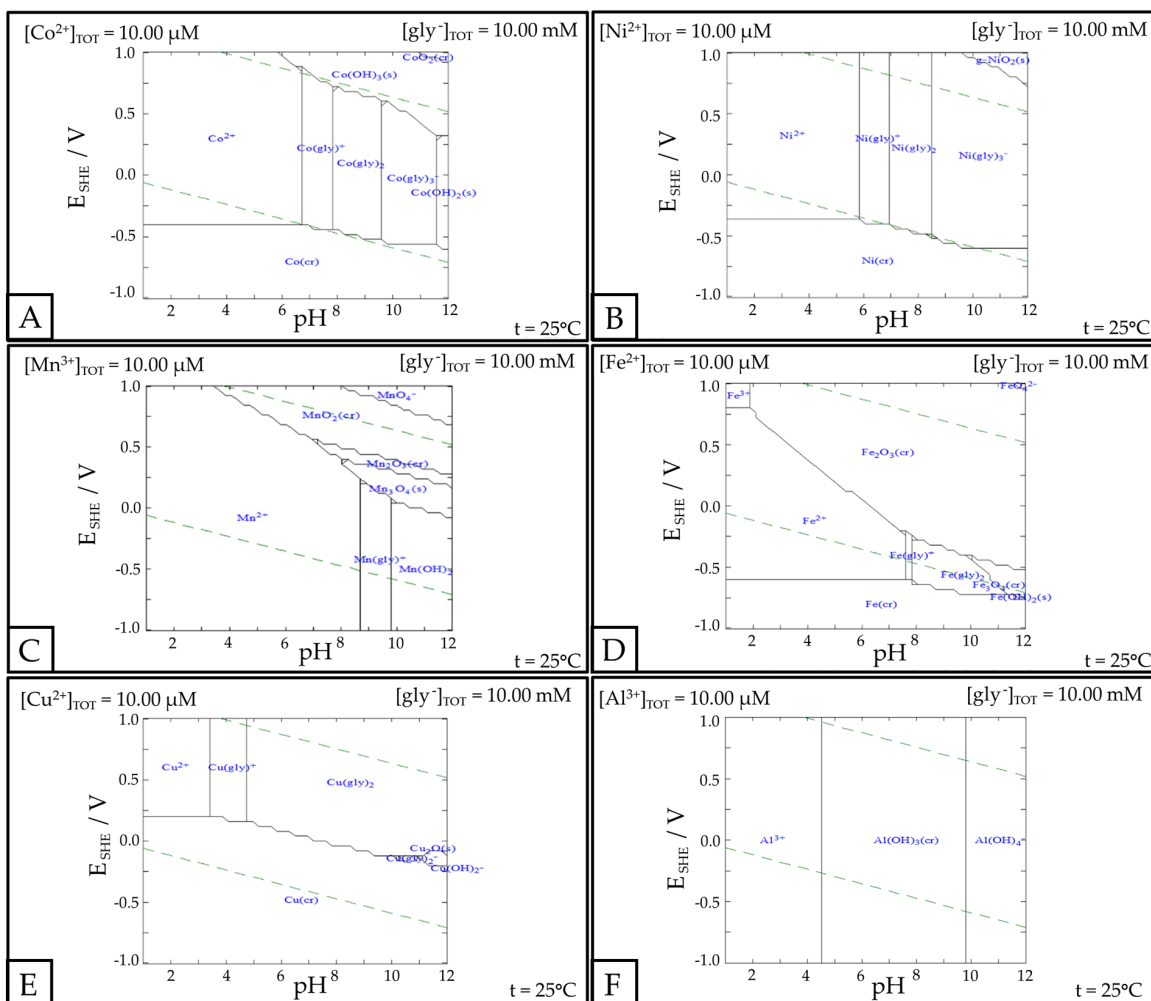


Figure 10. Eh vs. pH predominance diagrams for different metal–glycinate leaching systems, namely, Co (**A**), Ni (**B**), Mn (**C**), Fe (**D**), Cu (**E**), and Al (**F**).

3.5. Effect of Glycine Concentration—Industrial Black Mass

The glycine concentration was varied from 30 g/L to 100 g/L, while keeping other leaching parameters constant (2% solids, 60 °C, and an agitation speed of 600 rpm for 2 h). The results are presented in Figure 11A–E.

Leaching with a glycine concentration of 30 g/L (Figure 11A) was very selective toward Co, Ni, and Mn, with metal extractions after 2 h reaching 91.99%, 69.90%, and 35.77%, respectively. Minimal co-extractions of Cu, Fe, and Al were observed with 12.05%, 2.2%, and 1.89%, respectively. As the glycine concentration increased to 45 g/L (Figure 11B), there was no change in the amount of Co extracted; however, the extractions of Ni, Mn, and Cu increased to 80.41%, 47.43%, and 62.98%. The increase in Ni, Mn, and Cu extraction was due to the increased availability of glycine for metal dissolution. As the concentration of glycine increased to 60 g/L and, further, to 100 g/L, the amount of Co and Ni extracted (after 2 h) remained between 90–92% and 78–79%, respectively. These results illustrate just how stable the Co- and Ni-glycine complexes were over a large concentration range. The greatest change was observed in the amount of Fe and Mn being extracted. At 30 g/L of glycine, 2.2% of the Fe and 35.77% of the Mn were reported to be in the solution. However, when operating at 100 g/L, the amount of Mn and Fe being extracted increased to 71.80% and 80.51% after 2 h. These observations are clearly presented in Figure 11E, which illustrates that as the glycine concentration increased, the presence of more glycine resulted in an increase in the co-extraction of Mn, Fe, Cu, and Al, and, secondly, improved

the stability of the different metal–glycine complexes. This was particularly evident when examining the levels of Fe and Al in the leachate at the 2 h mark, as their presence in the solution only started to decrease after 3 h (see Appendix A). The results presented in Figures 10D and 11A–C and Appendix A illustrate that it was possible to reduce the amount of Fe being co-extracted, as with time, the Fe/Fe-glycinate became unstable and precipitated out of the pregnant leach solution as Fe_2O_3 and FeOOH . Overall, it can be concluded that in order to maintain selectivity toward Co, Ni, and Mn, glycine leaching should be conducted at 30 g/L for 2 h, as this minimizes co-extraction of Al, Fe, and Cu.

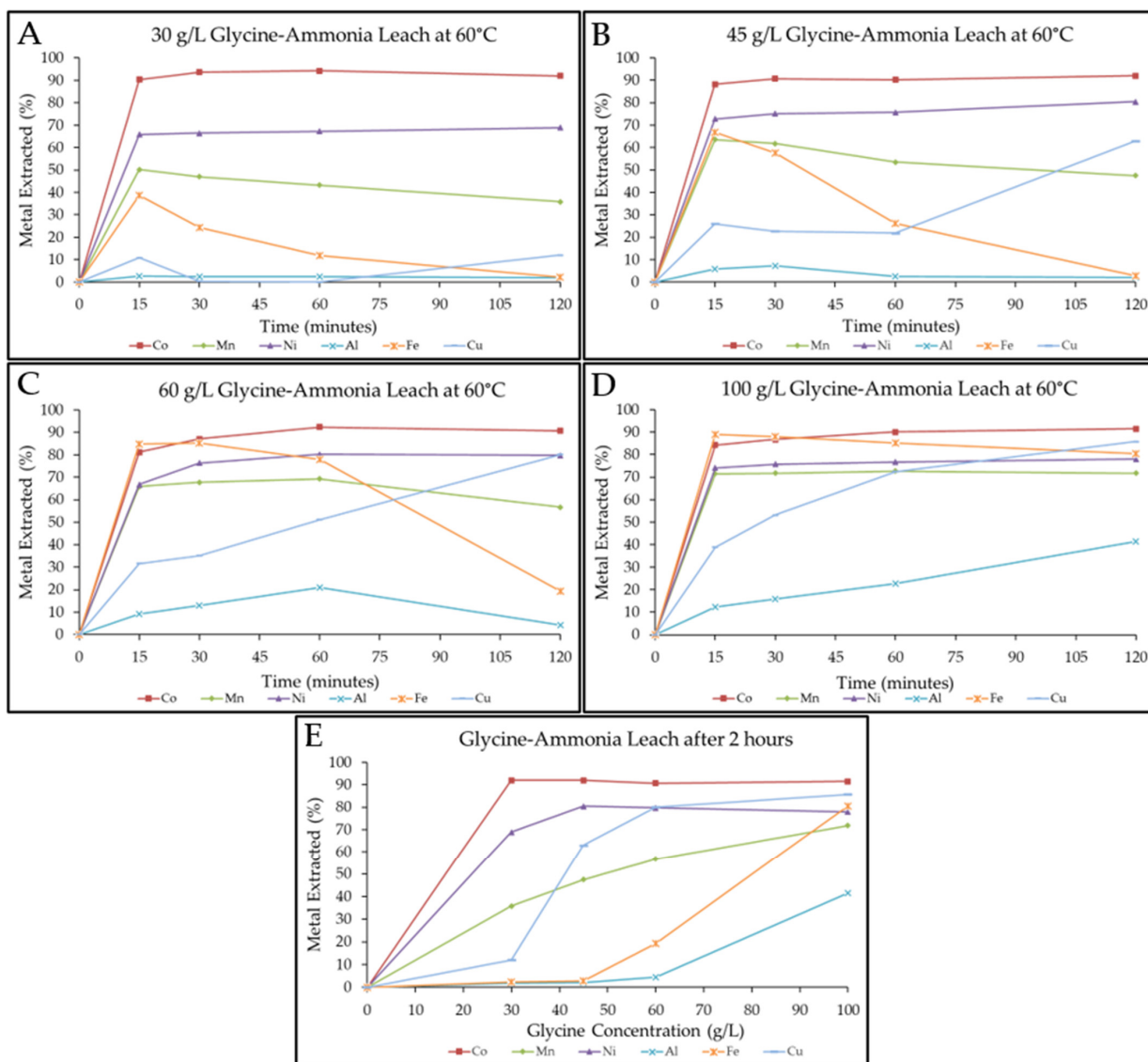


Figure 11. The effect of glycine concentration on metal extraction when leaching industrial black mass ($60\text{ }^{\circ}\text{C}$, 2% solids, and agitation rate of 600 rpm for 2 h), namely, 30 g/L (A), 40 g/L (B), 60 g/L (C), and 100 g/L (D). The effect of temperature on metal extraction after a 2 h leach (E).

3.6. Effect of Temperature on Glycine Leaching—Industrial Black Mass

The effect of temperature, varied from $25\text{ }^{\circ}\text{C}$ to $60\text{ }^{\circ}\text{C}$, on metal extraction was studied, and the results are presented in Figure 12A–D. All experiments were conducted using 30 g/L of glycine, with 2% solids, at an agitation rate of 600 rpm over a 2 h period. Figure 12A–C illustrate that within the first 15 min, as the temperature increased from $25\text{ }^{\circ}\text{C}$ to $60\text{ }^{\circ}\text{C}$, the extraction of Co and Ni increased from 86.31% and 61.95% to 90.42% and 68.90%. However, the co-extraction of the Mn, Fe, Cu, and Al decreased with an increase in

temperature, as the glycine–metal complexes became less stable, and insoluble metal hydroxides and metal oxides precipitated out of solution. This is evident when investigating the Eh–pH diagrams (see Figure 10C–F) for Al, Fe, Mn, and Cu, as at around pH 9–10, there were regions that favored the formation of different metal hydroxides and oxides. Overall (see Figure 12D), there was a small increase in Co, Ni, and Mn from 25 °C to 40 °C; however, the extraction decreased as the temperature increased further to 60 °C. These findings align with the work of [20], which reported a decrease in Co and Ni extractions when increasing the leaching temperature from 25 °C to 55 °C. Li and coworkers [23] concluded that at elevated temperatures (i.e., >55 °C), glycine decomposed through deamination and decarboxylation. This decomposition of glycine explains why there was a sudden drop across all metal species when the leaching temperature increased from 40 °C to 60 °C. Thus, if this process is conducted at an industrial scale, it is important from both an extraction efficiency and a reagent cost point of view to keep the leach at a temperature below 55 °C.

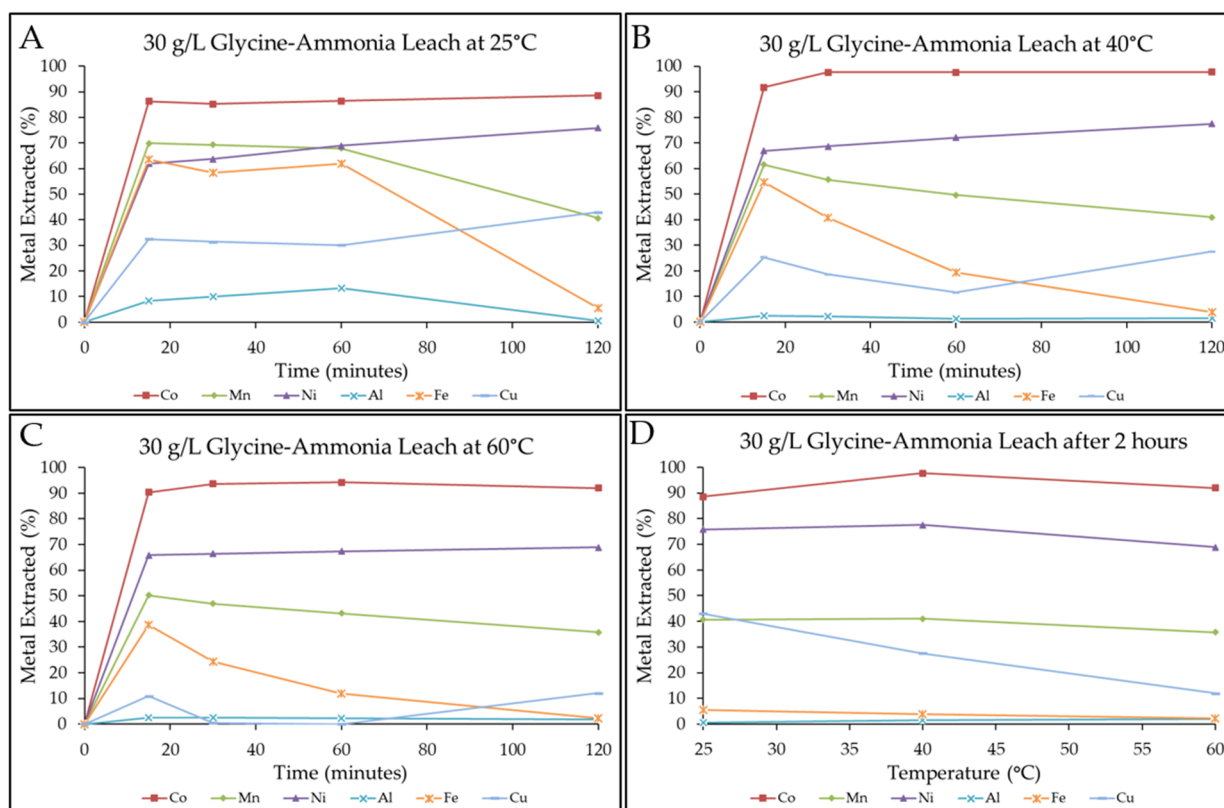


Figure 12. Effect of changing temperature on metal extraction during glycine leaching (30 g/L of glycine, with an agitation speed of 600 rpm, for 2 h, at 2% solids), when leaching at 25 °C (A), 40 °C (B), and 60 °C (C). Effect of temperature on metal extraction after a 2 h leach (D).

3.7. Industrial Applications

The main aims of this research were, firstly, to determine whether the leaching conditions identified in Henderson et al.’s study [13] could be applied to an industrially sourced mixed-chemistry BM, and, secondly, to identify a second-stage leaching step capable of selectively leaching Co, Ni, and Mn from the first-stage oxalic acid leach residue. Overall, this research has demonstrated (see Figure 13) the following:

- Oxalic acid is capable of selectively removing Al, Li, and P from a mixed-chemistry black mass, with extractions reaching >99% for Li and P and as high as 97% for Al.
- The co-extraction of Mn, Fe, Cu, Co, and Ni was low, with respective extractions of 19%, <3%, <1%, 0%, and 0%.

- The oxalic acid leach residue could be subsequently leached using a glycine–ammonia system, with ammonia for pH adjustment to around 9.6, in which >97% of the Co, >77% of the Ni, and 41% of the Mn could be extracted.

However, the greatest limitation of the oxalic acid leaching system is the solubility of oxalic acid (approximately 1.2 M at room temperature). If it is to be used at an industrial scale, careful consideration (i.e., leaching temperatures) must be given to operating at high oxalic acid concentrations, as alkali oxalates are easily precipitated out of the solution and, thus, cause scaling of equipment. The glycine leach is effective for the selective extraction of high-value Ni and Co from insoluble oxalates, while minimizing any co-extraction of Al and Fe. The second-stage leach needs to be further optimized to achieve >90% Ni and Co extractions; however, these initial findings are promising. Overall, when leaching using traditional inorganic acids, namely, H_2SO_4 , HNO_3 , and H_3PO_4 , large quantities of toxic off-gases (e.g., SO_3 and NO_x) and highly acidic SO_4^{2-} , NO_3^- , and PO_4^{3-} -containing waste streams are produced [50,51]. Therefore, the use of oxalic acid and glycine as lixivants will greatly reduce the production of the aforementioned harmful waste streams, aiding in industries' move toward the development of green hydrometallurgical recycling routes.

When considering treating pregnant leach solutions, researchers such as Li et al. [52] and Mohammed et al. [53] identified methods capable of selectively removing/recovering metals from oxalate and glycine leach solutions, respectively. Li and coworkers [52] determined that KOH would be best to promote Al precipitation, as when K^+ reacts with $C_2O_4^{2-}$, $K_2C_2O_4$ is formed, which is highly soluble. This is more desirable than using traditional pH modifiers such as NaOH, as the resultant $Na_2C_2O_4$ is far more insoluble than $K_2C_2O_4$; thus, it is more likely to precipitate out along with the $Al(OH)_3$. As determined by Li et al. [52], K_2CO_3 was used to recover >76% of the Li as Li_2CO_3 (>99% purity). Finally, Mohammed and coworkers [53] proved that a multistage solvent extraction stage, followed by H_2SO_4 stripping, allows for the selective recovery of Co, Cu, and Ni as sulfate solutions.

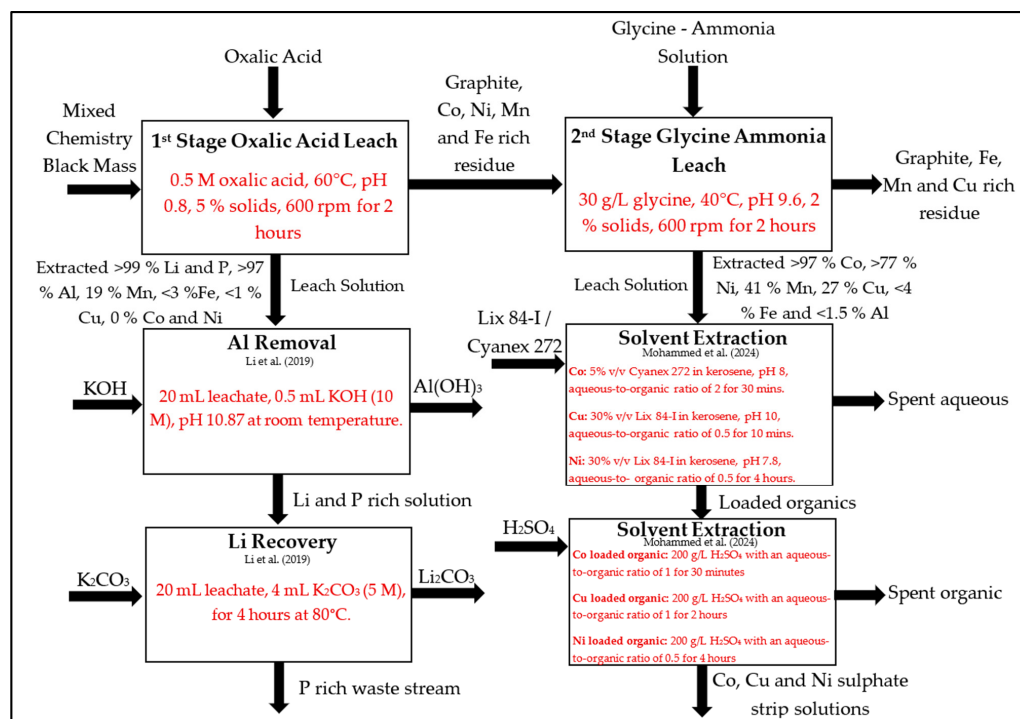


Figure 13. Two-stage leaching circuit for the selective leaching of industrially sourced black mass (Li et al. (2019) [52]; Mohammed et al. (2024) [53]).

4. Conclusions

This study has proven that the oxalic leaching process, developed for leaching a synthetic LFP-NMC 111 BM [13], can be used to selectively target LFP battery chemistries from an LFP-rich industrially sourced black mass. The Li and P extraction was markedly less, as the industrial black mass contained Al, which was co-extracted. The leaching process had to be optimized for the industrial sample. When leaching at the optimal parameters, identified in this research (0.5 M oxalic acid, 5% solids, pH 0.80, and agitation at 600 rpm at 60 °C for 2 h), it was concluded that >99% of the Li and P and >97% of the Al could be selectively extracted with approximately 19%, <3%, <1%, 0%, and 0% of the Mn, Fe, Cu, Ni, and Co being co-extracted. The greatest limitation was identified to be the solubility of oxalic acid at room temperature, and thus, if operating at high solid-to-liquid ratios (i.e., 10%), the leaching temperature is critical to prevent precipitation and scaling of leaching equipment.

This study further identified a second-stage leaching process capable of extracting and treating the oxalic leach residue. It was determined that glycine–ammonia can be used to selectively leach the Co– and Ni–oxalates from the leach residue. The second-stage glycine leach was not been fully optimized; however, under the partially optimized conditions (30 g/L glycine, pH 9.6, and agitation at 600 rpm at 40 °C for 2 h), it was concluded that >97% of the Co, >77% of the Ni, and 41% of the Mn was extracted, with 27%, <4%, and <1.5% of the Cu, Fe, and Al being co-extracted, respectively. The glycine concentration was observed to have a large effect on the co-extraction of Mn, Cu, Fe, and Al. The leaching temperatures that can be employed for glycine leaching should be kept below 55 °C, as at temperatures above 55 °C, metal extractions decrease due to the decomposition of glycine.

5. Considerations for Future Work

- Investigate whether higher-pH (4–7) oxalic acid leaching systems can be optimized to enhance the selective extraction of Co, Ni, and Mn.
- Optimize the second-stage glycine leaching system to achieve Co and Ni extractions of >90%, while minimizing the co-extraction of Fe and Al.
- Investigate whether a multistage glycine leaching step could be implemented to first leach the Co and Ni at low glycine concentrations and then leach Mn and Cu at higher glycine concentrations.
- Investigate whether it is possible to add a complexing agent to the glycine leaching stage to reduce the co-extraction of Mn and Fe.
- Investigate the scaling effect of oxalic acid on leaching reactors and identify ways in which to reduce scaling when using high oxalic acid concentrations.

Author Contributions: Conceptualization, J.E., E.A.O., C.C.B. and M.S.H.; methodology, M.S.H., E.A.O., J.E. and C.C.B.; validation, M.S.H.; formal analysis, M.S.H.; ICP-OES was conducted by M.S.H.; SEM imaging was conducted by M.S.H.; investigation, M.S.H.; resources, J.E., E.A.O. and C.C.B.; data curation, M.S.H.; writing—original draft preparation, M.S.H.; writing—review and editing, M.S.H., C.C.B. and E.A.O.; data visualization, M.S.H.; supervision, J.E., E.A.O. and C.C.B.; project administration, J.E., E.A.O., C.C.B. and M.S.H.; funding acquisition, J.E., E.A.O. and C.C.B. All authors have read and agreed to the published version of the manuscript.

Funding: The Future Battery Industries CRC (FBI-CRC, as part of the Australian Government Cooperative Research Centers Program) and Curtin University funded the staff salaries and fee scholarships (for Marc Henderson). Part of this research was undertaken using the Tescan Clara FESEM with Oxford instrumentation (ARC LE 190100176) at the John de Laeter Centre, Curtin University. The black mass samples were provided by Envirostream, a wholly owned subsidiary of Livium Ltd.

Data Availability Statement: The data presented in this study are available on request from the corresponding author on reasonable request.

Conflicts of Interest: The authors declare no conflicts of interest. The authors declare that this study received funding from Envirostream, BASF and BHP. The funders were not involved in the study design, collection, analysis, interpretation of data or the writing of this article.

Appendix A

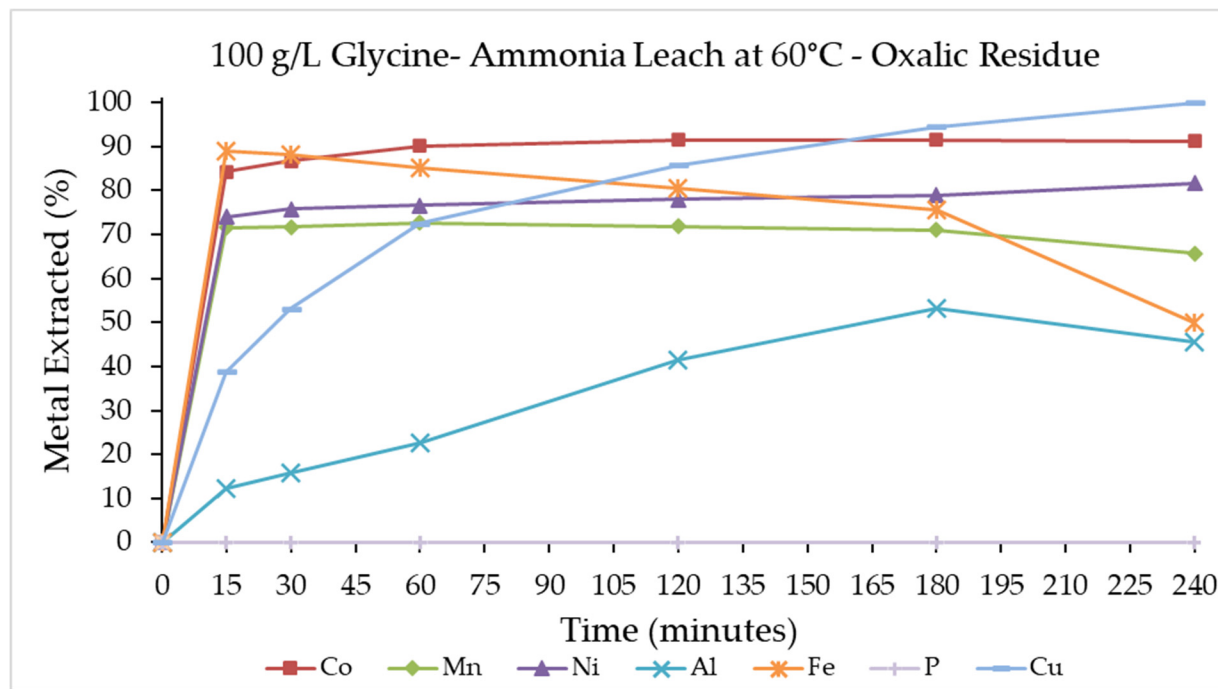


Figure A1. Continuation of Figure 11D: 4 h glycine–ammonia leach of oxalic leach residue.

References

- Li, Q.; Fung, K.Y.; Xu, L.; Wibowo, C.; Ng, K.M. Process Synthesis: Selective Recovery of Lithium from Lithium-Ion Battery Cathode Materials. *Ind. Eng. Chem. Res.* **2019**, *58*, 3118–3130. [[CrossRef](#)]
- Choi, J.W.; Kim, J.; Kim, S.K.; Yun, Y.S. Simple, green organic acid-based hydrometallurgy for waste-to-energy storage devices: Recovery of NiMnCoC₂O₄ as an electrode material for pseudocapacitor from spent LiNiMnCoO₂ batteries. *J. Hazard. Mater.* **2022**, *424 Pt B*, 127481. [[CrossRef](#)]
- Sun, L.; Qiu, K. Organic oxalate as leachant and precipitant for the recovery of valuable metals from spent lithium-ion batteries. *Waste Manag.* **2012**, *32*, 1575–1582. [[CrossRef](#)] [[PubMed](#)]
- Rouquette, L.M.J.; Petranikova, M.; Vieceli, N. Complete and selective recovery of lithium from EV lithium-ion batteries: Modeling and optimization using oxalic acid as a leaching agent. *Sep. Purif. Technol.* **2023**, *320*, 124143. [[CrossRef](#)]
- Saleem, U.; Buvik, V.; Knuutila, H.K.; Bandyopadhyay, S. Recovery of lithium from oxalic acid leachate produced from black mass of spent electric vehicle Li-ion batteries. *Chem. Eng. J. Adv.* **2024**, *20*, 100648. [[CrossRef](#)]
- Gerold, E.; Kadisch, F.; Lerchammer, R.; Antrekowitsch, H. Bio-metallurgical recovery of lithium, cobalt, and nickel from spent NMC lithium ion batteries: A comparative analysis of organic acid systems. *J. Hazard. Mater. Adv.* **2024**, *13*, 100397. [[CrossRef](#)]
- Mettke, L.N.; Yagmurlu, B. Optimizing Early-Stage Lithium Recovery: Investigating Oxalic Acid Leaching of Black Mass from End-of-Life NMC 622 Batteries. In *REWAS 2025, Proceedings of the TMS Annual Meeting & Exhibition, Las Vegas, NV, USA, 23–27 March 2025*; Lazou, A., Meskers, C., Olivetti, E., Diaz, F., Gökelma, M., Eds.; Springer: Cham, Switzerland, 2025; pp. 13–22.
- Verma, A.; Kore, R.; Corbin, D.R.; Shiflett, M.B. Metal Recovery Using Oxalate Chemistry: A Technical Review. *Ind. Eng. Chem. Res.* **2019**, *58*, 15381–15393. [[CrossRef](#)]
- Müller, M.; Yagmurlu, B. Synergistic Processing of Mixed LFP-NMC Black Mass for Improved Recycling Operations. In *REWAS 2025, Proceedings of the TMS Annual Meeting & Exhibition, Las Vegas, NV, USA, 23–27 March 2025*; Lazou, A., Meskers, C., Olivetti, E., Diaz, F., Gökelma, M., Eds.; Springer: Cham, Switzerland, 2025; pp. 43–53.

10. Zhao, T.; Traversy, M.; Choi, Y.; Ghahreman, A. A novel process for multi-stage continuous selective leaching of lithium from industrial-grade complicated lithium-ion battery waste. *Sci. Total Environ.* **2024**, *909*, 168533. [[CrossRef](#)]
11. Zou, Y.; Chernyaev, A.; Ossama, M.; Seisko, S.; Lundstrom, M. Leaching of NMC industrial black mass in the presence of LFP. *Sci. Rep.* **2024**, *14*, 10818. [[CrossRef](#)]
12. Vieceli, N.; Benjamasutin, P.; Promphan, R.; Hellström, P.; Paulsson, M.; Petranikova, M. Recycling of Lithium-Ion Batteries: Effect of Hydrogen Peroxide and a Dosing Method on the Leaching of LCO, NMC Oxides, and Industrial Black Mass. *ACS Sustain. Chem. Eng.* **2023**, *11*, 9662–9673. [[CrossRef](#)]
13. Henderson, M.S.; Beh, C.C.; Oraby, E.; Eksteen, J. Organic Acid Leaching of Black Mass with an LFP and NMC Mixed Chemistry. *Recycling* **2025**, *10*, 145. [[CrossRef](#)]
14. Refly, S.; Floweri, O.; Mayangsari, T.R.; Sumboja, A.; Santosa, S.P.; Ogi, T.; Iskandar, F. Regeneration of $\text{LiNi}_{1/3}\text{Co}_{1/3}\text{Mn}_{1/3}\text{O}_2$ Cathode Active Materials from End-of-Life Lithium-Ion Batteries through Ascorbic Acid Leaching and Oxalic Acid Coprecipitation Processes. *ACS Sustain. Chem. Eng.* **2020**, *8*, 16104–16114. [[CrossRef](#)]
15. Choi, J.W.; Cho, C.W.; Yun, Y.S. Organic acid-based linear free energy relationship models for green leaching of strategic metals from spent lithium-ion batteries and improvement of leaching performance. *J. Hazard. Mater.* **2022**, *423 Pt B*, 127214. [[CrossRef](#)]
16. Musariri, B.; Akdogan, G.; Dorfling, C.; Bradshaw, S. Evaluating organic acids as alternative leaching reagents for metal recovery from lithium ion batteries. *Miner. Eng.* **2019**, *137*, 108–117. [[CrossRef](#)]
17. Schmitz, D.; Prasetyo, H.; Birich, A.; Yeetsorn, R.; Friedrich, B. Co-Precipitation of Metal Oxalates from Organic Leach Solution Derived from Spent Lithium-Ion Batteries (LIBs). *Metals* **2024**, *14*, 80. [[CrossRef](#)]
18. Zhang, J.; Hu, X.; He, T.; Yuan, X.; Li, X.; Shi, H.; Yang, L.; Shao, P.; Wang, C.; Luo, X. Rapid extraction of valuable metals from spent $\text{LiNi}_x\text{Co}_y\text{Mn}_{1-x-y}\text{O}_2$ cathodes based on synergistic effects between organic acids. *Waste Manag.* **2023**, *165*, 19–26. [[CrossRef](#)] [[PubMed](#)]
19. Zhang, J.; Ding, Y.; Shi, H.; Shao, P.; Yuan, X.; Hu, X.; Zhang, Q.; Zhang, H.; Luo, D.; Wang, C.; et al. Selective recycling of lithium from spent $\text{LiNi}_x\text{Co}_y\text{Mn}_{1-x-y}\text{O}_2$ cathode via constructing a synergistic leaching environment. *J. Environ. Manag.* **2024**, *352*, 120021. [[CrossRef](#)]
20. Eksteen, J.J.; Oraby, E.A.; Nguyen, V. Leaching and ion exchange based recovery of nickel and cobalt from a low grade, serpentine-rich sulfide ore using an alkaline glycine lixiviant system. *Miner. Eng.* **2020**, *145*, 106073. [[CrossRef](#)]
21. Oraby, E.; Li, H.; Deng, Z.; Eksteen, J. Selective extraction of Ni and Co from a pyrrhotite-rich flotation slime using an alkaline glycine-based leach system. *Miner. Eng.* **2023**, *203*, 108330. [[CrossRef](#)]
22. Oraby, E.; Deng, Z.; Li, H.; Eksteen, J. Selective extraction of nickel and cobalt from disseminated sulfide flotation cleaner tailings using alkaline glycine-ammonia leaching solutions. *Miner. Eng.* **2023**, *204*, 108418. [[CrossRef](#)]
23. Li, H.; Oraby, E.; Eksteen, J. Extraction of copper and the co-leaching behaviour of other metals from waste printed circuit boards using alkaline glycine solutions. *Resour. Conserv. Recycl.* **2020**, *154*, 104624. [[CrossRef](#)]
24. Chen, M.; Wang, R.; Qi, Y.; Han, Y.; Wang, R.; Fu, J.; Meng, F.; Yi, X.; Huang, J.; Shu, J. Cobalt and lithium leaching from waste lithium ion batteries by glycine. *J. Power Sources* **2021**, *482*, 228942. [[CrossRef](#)]
25. Wang, F.; Sun, R.; Xu, J.; Chen, Z.; Kang, M. Recovery of cobalt from spent lithium ion batteries using sulphuric acid leaching followed by solid–liquid separation and solvent extraction. *RSC Adv.* **2016**, *6*, 85303–85311. [[CrossRef](#)]
26. Nayl, A.A.; Elkhashab, R.A.; Badawy, S.M.; El-Khateeb, M.A. Acid leaching of mixed spent Li-ion batteries. *Arab. J. Chem.* **2017**, *10*, S3632–S3639. [[CrossRef](#)]
27. Li, H.; Xing, S.; Liu, Y.; Li, F.; Guo, H.; Kuang, G. Recovery of Lithium, Iron, and Phosphorus from Spent LiFePO_4 Batteries Using Stoichiometric Sulfuric Acid Leaching System. *ACS Sustain. Chem. Eng.* **2017**, *5*, 8017–8024. [[CrossRef](#)]
28. Zhang, X.; Bian, Y.; Xu, S.; Fan, E.; Xue, Q.; Guan, Y.; Wu, F.; Li, L.; Chen, R. Innovative Application of Acid Leaching to Regenerate $\text{Li}(\text{NiCoMn})\text{O}_2$ Cathodes from Spent Lithium-Ion Batteries. *ACS Sustain. Chem. Eng.* **2018**, *6*, 5959–5968. [[CrossRef](#)]
29. Li, L.; Lu, J.; Zhai, L.; Zhang, X.; Curtiss, L.; Jin, Y.; Wu, F.; Chen, R.; Amine, K. A facile recovery process for cathodes from spent lithium iron phosphate batteries by using oxalic acid. *CSEE J. Power Energy Syst.* **2018**, *4*, 219–225. [[CrossRef](#)]
30. Haynes, W.M.; Lide, D.R.; Bruno, T.J. *CRC Handbook of Chemistry and Physics*, 97th ed.; CRC Press Taylor and Francis Group: Boco Raton, FL, USA, 2017.
31. Liu, F.; Peng, C.; Wilson, B.P.; Lundström, M. Oxalic Acid Recovery from High Iron Oxalate Waste Solution by a Combination of Ultrasound-Assisted Conversion and Cooling Crystallization. *ACS Sustain. Chem. Eng.* **2019**, *7*, 17372–17378. [[CrossRef](#)]
32. Liu, J.; Lin, J.; Yin, Z.; Tong, Z.; Liu, J.; Wang, Z.; Zhou, Y.; Li, J. Electrocatalytic Decomposition of Lithium Oxalate-Based Composite Microspheres as a Prelithiation Additive in Lithium-Ion Batteries. *Molecules* **2024**, *29*, 2975. [[CrossRef](#)]
33. Li, W.; Wang, N.; Lu, F.; Chai, H.; Gu, H. Selective separation of aluminum, silicon, and titanium from red mud using oxalic acid leaching, iron precipitation and pH adjustments with calcium carbonate. *Hydrometallurgy* **2024**, *223*, 106221. [[CrossRef](#)]
34. Hussaini, S.; Tita, A.M.; Kursunoglu, S.; Kaya, M.; Chu, P. Leaching of Nickel and Cobalt from a Mixed Nickel-Cobalt Hydroxide Precipitate Using Organic Acids. *Minerals* **2024**, *14*, 314. [[CrossRef](#)]

35. Xuan, W.; de Souza Braga, A.; Korbel, C.; Chagnes, A. New insights in the leaching kinetics of cathodic materials in acidic chloride media for lithium-ion battery recycling. *Hydrometallurgy* **2021**, *204*, 105705. [[CrossRef](#)]
36. Liu, Y.; Zhang, C.; Li, B.; Li, H.; Zhan, H. Extraction and Determination of Total and Soluble Oxalate in Pulping and Papermaking Raw Materials. *BioResources* **2015**, *10*, 4580–4587. [[CrossRef](#)]
37. Redox Ltd. *Safety Data Sheet Oxalic Acid, Dihydrate*; Redox Ltd.: Sydney, Australia, 2025; 11p.
38. Zeng, X.; Li, J.; Shen, B. Novel approach to recover cobalt and lithium from spent lithium-ion battery using oxalic acid. *J. Hazard. Mater.* **2015**, *295*, 112–118. [[CrossRef](#)]
39. Lie, J.; Liu, J.-C. Closed-vessel microwave leaching of valuable metals from spent lithium-ion batteries (LIBs) using dual-function leaching agent: Ascorbic acid. *Sep. Purif. Technol.* **2021**, *266*, 118458. [[CrossRef](#)]
40. Nayaka, G.P.; Manjanna, J.; Pai, K.V.; Vadavi, R.; Keny, S.J.; Tripathi, V.S. Recovery of valuable metal ions from the spent lithium-ion battery using aqueous mixture of mild organic acids as alternative to mineral acids. *Hydrometallurgy* **2015**, *151*, 73–77. [[CrossRef](#)]
41. Broeksma, C.P.; Dorfling, C. Evaluating glycine as an alternative lixiviant for copper recovery from waste printed circuit boards. *Waste Manag.* **2023**, *163*, 96–107. [[CrossRef](#)]
42. Rezaee, M.; Saneie, R.; Mohammadzadeh, A.; Abdollahi, H.; Kordloo, M.; Rezaee, A.; Vahidi, E. Eco-friendly recovery of base and precious metals from waste printed circuit boards by step-wise glycine leaching: Process optimization, kinetics modeling, and comparative life cycle assessment. *J. Clean. Prod.* **2023**, *389*, 136016. [[CrossRef](#)]
43. Rautela, R.; Yadav, B.R.; Kumar, S. Enhancing the efficiency of metals extraction from waste lithium-ion batteries through glycine leaching using response surface methodology for economic feasibility. *J. Clean. Prod.* **2024**, *447*, 141602. [[CrossRef](#)]
44. Tanda, B.C.; Eksteen, J.J.; Oraby, E.A.; O'Connor, G.M. The kinetics of chalcopyrite leaching in alkaline glycine/glycinate solutions. *Miner. Eng.* **2019**, *135*, 118–128. [[CrossRef](#)]
45. Cuculić, V.; Pižeta, I. Kinetics of iron(III) hydrolysis and precipitation in aqueous glycine solutions assessed by voltammetry. *Collect. Czechoslov. Chem. Commun.* **2009**, *74*, 1531–1542. [[CrossRef](#)]
46. Casale, A.; De Robertis, A.; De Stefano, C.; Gianguzza, A.; Patane, G.; Rigano, C. Thermodynamic parameters for the formation of glycine complexes with magnesium(II), calcium(II), lead(II), manganese(II), cobalt(II), nickel(II), zinc(II) and cadmium(II) at different temperatures and ionic strengths, with particular reference to natural fluid conditions. *Thermochim. Acta* **1995**, *255*, 109–141.
47. Cuculić, V.; Pižeta, I.; Branica, M. Voltammetric determination of stability constants of iron(III)-glycine complexes in water solution. *J. Electroanal. Chem.* **2005**, *583*, 140–147. [[CrossRef](#)]
48. Kiss, T.; Sovago, I.; Gergely, A. Critical survey of stability constants of complexes of glycine. *Pure Appl. Chem.* **1991**, *63*, 597–638. [[CrossRef](#)]
49. Blais, J.F.; Djedidi, Z.; Cheikh, R.B.; Tyagi, R.D.; Mercier, G. Metals Precipitation from Effluents: Review. *Pract. Period. Hazard. Toxic Radioact. Waste Manag.* **2008**, *12*, 135–149. [[CrossRef](#)]
50. Wu, Z.; Soh, T.; Chan, J.J.; Meng, S.; Meyer, D.; Srinivasan, M.; Tay, C.Y. Repurposing of Fruit Peel Waste as a Green Reductant for Recycling of Spent Lithium-Ion Batteries. *Environ. Sci. Technol.* **2020**, *54*, 9681–9692. [[CrossRef](#)] [[PubMed](#)]
51. Meshram, P.; Mishra, A.; Abhilash; Sahu, R. Environmental impact of spent lithium ion batteries and green recycling perspectives by organic acids—A review. *Chemosphere* **2020**, *242*, 125291. [[CrossRef](#)]
52. Li, Q.; Fung, K.Y.; Ng, K.M. Hydrometallurgy process for the recovery of valuable metals from $\text{LiNi}_{0.8}\text{Co}_{0.15}\text{Al}_{0.05}\text{-O}_2$ cathode materials. *SN Appl. Sci.* **2019**, *1*, 690. [[CrossRef](#)]
53. Mohammed, T.; Bezuidenhout, G.A.; Oraby, E.A.; Eksteen, J.J. Sequential Separation of Cobalt, Copper, and Nickel from Alkaline Glycinate Solutions Using Solvent Extraction. *J. Sustain. Metall.* **2024**, *10*, 2455–2468. [[CrossRef](#)]

Disclaimer/Publisher's Note: The statements, opinions and data contained in all publications are solely those of the individual author(s) and contributor(s) and not of MDPI and/or the editor(s). MDPI and/or the editor(s) disclaim responsibility for any injury to people or property resulting from any ideas, methods, instructions or products referred to in the content.